

# Weak axial nuclear heavy meson exchange currents and interactions of solar neutrinos with deuterons

B. Mosconi

*Università di Firenze, Department of Physics,  
and Istituto Nazionale di Fisica Nucleare, Sezione di Firenze,  
I-50019, Sesto Fiorentino (Firenze), Italy*

P. Ricci

*Istituto Nazionale di Fisica Nucleare, Sezione di Firenze,  
I-50019, Sesto Fiorentino (Firenze), Italy*

E. Truhlík

*Institute of Nuclear Physics ASCR, CZ-250 68 Řež, Czech Republic*

## Abstract

Starting from the axial heavy meson exchange currents, constructed earlier in conjunction with the Bethe–Salpeter equation, we first present the axial  $\rho^-$ ,  $\omega^-$  and  $a_1$  meson exchange Feynman amplitudes that satisfy the partial conservation of the axial current. Employing these amplitudes, we derive the corresponding weak axial heavy meson exchange currents in the leading order in the  $1/M$  expansion ( $M$  is the nucleon mass), suitable for the nuclear physics calculations beyond the threshold energies and with wave functions obtained by solving the Schrödinger equation with one–boson exchange potentials. The constructed currents obey the nuclear form of the partial conservation of the axial current. We apply the space component of these currents in calculations of the cross sections for the disintegration of deuterons by low energy (anti)neutrinos. The deuteron and the final state nucleon–nucleon wave functions are derived (i) from a variant of the OBEPQB potential, and (ii) from the Nijmegen 93 and Nijmegen I nucleon–nucleon interaction. The extracted values of the constant  $L_{1,A}$ , entering the axial exchange currents of the pionless effective field theory, are in a reasonable agreement with its value predicted by the dimensional analysis.

PACS numbers: 11.40.Ha; 25.30.-c; 25.60.-t

Keywords: weak axial; nuclear; heavy meson; exchange current

## I. INTRODUCTION

Since quarks are confined, the quantum chromodynamics [1, 2] is not directly suitable for the investigation of nuclear physics phenomena at low and intermediate energies. Instead of quarks and gluons one employs effective degrees of freedom (hadrons), and ideas and methods based on the concept of the spontaneously broken chiral symmetry [3, 4]. The hadronic degrees of freedom, relevant for describing a nucleus and its response to the external electroweak interactions, are nucleon,  $\Delta(1236)$  isobar and low lying mesons at the hadron mass scale, like  $\pi^-$ ,  $\rho^-$ ,  $\omega^-$ ,... mesons. The interaction of the vector mesons with the baryons and pions is fixed by the vector dominance model (VDM) [5]. This concept has been developed successfully during the last 4 decades [6–11], and is called by some authors as the Standard Nuclear Physics Approach (SNPA) [12].

Starting from the early 1970s, a particular effort was devoted to the study of mesonic degrees of freedom in nuclei by investigating meson exchange currents (MECs) effects [13–21]. One of the best proofs of presence of the pionic degrees of freedom in nuclei follows from the study of the transition  $0^+ \leftrightarrow 0^-$  in the  $A=16$  nuclei [16, 21], induced by the time component of the axial current. Detailed studies have shown that the experimental data and the calculations can be reconciled only if the time component of the weak axial soft pion exchange current [14] is taken into account. The hard pion corrections [22, 23] change the result by 10-15 %. The time component of the weak axial MECs plays an important role also in interpreting the data on the isovector  $0^+ \leftrightarrow 1^+$  transition in the  $A=12$  nuclei [24] and on the  $0^+ \leftrightarrow 0^-$  transitions in medium-heavy and heavy nuclei. In these last transitions, the part of this component arising from the heavy meson exchanges, contributes sizeably [25–27]. The weak axial exchange charge densities, derived for the phenomena at the threshold, are given by pair terms that are related to nucleon–nucleon potentials [25], or are obtained from the chiral Lagrangian [26].

In the classification of Ref. [14], the leading term of the space component of the axial MECs of the pion range is of the order  $\sim \mathcal{O}(1/M^2)$ , where  $M$  is the nucleon mass. Being of relativistic origin, it is model dependent. This component of the weak axial MECs plays an important role in such fundamental reactions as

- (i) the neutrino reactions in nuclei at low and intermediate energies,
- (ii) the weak transitions in light nuclei, in particular the tritium beta decay, ordinary muon capture in  $^2\text{H}$  and  $^3\text{He}$  \*, and the solar fusion  $pp$  and  $p^3\text{He}$  processes, so important for the determination of the flux of the solar neutrinos,
- (iii) and the parity violating (PV) electron scattering that aims at elucidating the strange quark contribution to the electromagnetic structure of the nucleon †.

With the use of the chiral Lagrangians, the structure of the space component of the weak axial MECs of the pion range was studied in detail in the hard pion model [38] in Refs. [18, 39, 40], and applied to various reactions in the lightest nuclei [39, 41–43]. The largest effect arises from the  $\Delta$  excitation current of the pion range, that is partially compensated by the analogous current of the  $\rho$  meson range. Besides, the pair current of the  $\rho$  meson range was used during the last decade in Refs. [12, 44]. However, the origin of its derivation remains

---

\* For the recent review on these two reactions see Refs. [28]–[30].

† Several calculations of the PV inclusive [31–35] and exclusive [36, 37] electron scattering off deuterons have already been done considering different theoretical issues, however, the axial exchange currents have not yet been included in the calculations.

unclear.

The method used in Ref. [25] for the construction of the axial charge at the threshold was applied in Ref. [45] to the derivation of the space component of the weak axial potential MECs.

The weak axial MECs of the  $N\pi\sigma\omega$  system have recently been studied in Ref. [46], employing the Lagrangian based on the linear  $\sigma$  model [47]. The model suffers from some problems discussed in detail in Ref. [48].

The weak axial MECs of the pion range in the Bethe–Salpeter approach to the nuclear two–body problem has been studied in various chiral models in Ref. [49]. Another recent construction of the weak axial one–boson exchange currents for the Bethe–Salpeter equation has been done in Ref. [50] making use of the chiral Lagrangians of the  $N\Delta\pi\rho\omega a_1$  system [38, 51]. The obtained current operators fulfill the Ward–Takahashi identities and the matrix element of the full current, sandwiched between the two–body solutions of the Bethe–Salpeter equation, satisfies the PCAC constraint.

The chiral Lagrangians [38, 51] are constructed in such a way [4, 38, 47, 51–56] that they reproduce results obtained from the current algebra and PCAC in the tree approximation. Besides possessing the chiral symmetry, our Lagrangians are characterized by the following properties: (i) They respect VDM, reproduce universality, KSFRI, KSFRII. (ii) They provide the correct anomalous magnetic moment of the  $a_1$  meson. (iii) They reproduce the current algebra prediction for the weak pion production amplitude. It was explicitly shown [51] for the Lagrangian, based on the hidden local symmetry approach that if the  $a_1$  meson field is eliminated, the resulting Lagrangian preserves the properties (i) and (iii). Moreover, if the  $\rho$  meson field is eliminated from this Lagrangian, the chiral Lagrangian of the nucleons and pions is recovered [57]. Hence our Lagrangians consistently combine the chiral approach with the VDM concept, and provide a reasonable approximation at the tree level to the hadron amplitudes up to the energy scale  $\approx 1\text{ GeV}$  ( $\approx m_\rho, m_{a_1}, M$ ). Subsequently, these Lagrangians were applied to the construction of the weak axial MECs in the tree approximation: the generic relativistic Feynman tree-level amplitudes satisfy the PCAC constraint and the nuclear MECs derived from them are required to satisfy the nuclear PCAC constraint (see below). In this approach, the weak hadron form factors are naturally of the VDM form, but the strong nucleon form factors should be introduced by hand.

In practical calculations, one makes the non–relativistic reduction of the currents by expanding in  $Q/M_h$ , where  $Q$  is the momentum of the external particles or the momentum transfer, and  $M_h$  is the heavy meson or nucleon mass. Besides the leading order terms, the leading relativistic corrections have been calculated in the electromagnetic sector for the MECs of the pion range [58, 59]. Due to the presence of the small expansion parameter, the model currents are expected to be valid in the energy/momentum region up to  $\approx 0.4\text{ GeV}$ . Let us note that the cross sections for the backward deuteron electrodisintegration calculated in [51] describe well the data up to  $Q^2 \approx 1.2\text{ (GeV/c)}^2$  [60, 61].

We shall call the above described approach, where the currents and potentials are constructed in the tree approximation, as Tree Approximation Approach (TAA). The advantage of this approach is a relative simplicity and transparency. On the other hand, the obtained results can be considered fully realistic. Moreover, the nuclear PCAC constraint connects a part of the axial nuclear MECs (potential MECs) with the nuclear potential derived within the same approach. Making use of this potential in the production of the nuclear wave functions, one can do consistent calculations of the potential MECs effect. Let us note that the problem with the consistency of the calculations is by most authors overlooked [62].

In principle, the TAA is improved by effective field theories (EFTs). An EFT is based on the most general Lagrangian involving the relevant degrees of freedom, and respecting chiral symmetry [1, 2, 63]. For the pion–nucleon system, this approach, that was developed intensively in the 1990s [64–66], inspired a burst of applications in the region of low energies [67]. In particular, the time component of the weak axial MECs of the pion–nucleon system was constructed [68] within the framework of the heavy baryon chiral perturbation theory. Besides the tree approximation, it contains the contribution from the one–loop graphs. It was subsequently applied [69] to the calculation of the MECs effect in nuclei that has already been discussed above.

The space component of the weak axial MECs of the pion–nucleon system was constructed within the same scheme in Ref. [70] and applied to the weak interaction processes in the lightest nuclei in Refs. [70–73]. These calculations are hybrid, since the MECs are taken from the EFT, whereas the nuclear wave functions are derived from the potential models of the SNPA. Moreover, as it has recently been discussed in [62], the long–range part of these MECs does not satisfy the nuclear PCAC constraint.

Another EFT [66] was applied to the construction of the space component of the weak axial MECs in Refs. [74, 75] where also its influence on the reactions of the low energy (anti)neutrinos in deuterons was investigated.

The validity of the EFTs, based on the nucleonic and pionic degrees of freedom and with the heavy meson and  $\Delta$  isobar degrees of freedom integrated out, is necessarily restricted to the long wave–length limit and internuclear distances  $r \geq 0.6$  fm [68]. It is natural that in parallel with the development and applications of these EFTs, attempts appeared [76] to construct a class of EFTs without this restriction. The  $\Delta$  isobar has already been included explicitly within the small scale expansion scheme [65] and it has recently been demonstrated in Ref. [77] that under certain conditions one can obtain a consistent power counting for model Lagrangians including vector mesons.

As it is seen from the discussion, a systematic derivation of the weak axial heavy MECs operator that would respect chiral symmetry and VDM is lacking. In the absence of an EFT including explicitly heavy mesons, we construct here such an operator from our chiral Lagrangians in the TAA. Using this operator in calculations of observables at low energies and comparing the results with the calculations based on existing EFTs and with the data can provide a test of soundness of our approach<sup>‡</sup>.

The main goal of this study should be seen in the construction of the weak axial nuclear exchange currents (WANECs) of the heavy meson range, suitable in the SNPA calculations beyond the long wave–length limit, with the nuclear wave functions generated from the Schrödinger equation and the related one–boson exchange potentials (OBEPs). For the construction of the WANECs we make use of the weak axial two–nucleon relativistic amplitudes derived in [50] to which we add the nucleon Born terms. The WANECs are then defined by analogy with the electromagnetic MECs [58, 78], as the difference between these relativistic amplitudes and the first Born iteration of the weak axial one–nucleon current contribution to the two–nucleon scattering amplitude satisfying the Lippmann–Schwinger equation. This method has already been applied in [39, 40, 62] to the construction of the weak axial MECs of the pion range. It can be shown in the same manner that the WANECs, defined in this

---

<sup>‡</sup> A test of this kind has recently been done in Ref. [12].

way, satisfy the nuclear PCAC equation of the type [79]

$$q_\mu A_\mu^a(2) = [V, A_0^a(1)] + i f_\pi m_\pi^2 \Delta_F^\pi(q^2) \mathcal{M}^a(2), \quad (1.1)$$

which follows, as is shortly discussed in appendix A, from the assumption that the axial current consists of one- and two-body terms and it satisfies the PCAC hypothesis for the total axial current. Therefore, these currents are suitable for calculations of observables for weak processes in the intermediate energy region exactly as the vector exchange currents satisfying the nuclear conserved vector current (CVC) equation

$$q_\mu V_\mu^a(2) = [V, V_0^a(1)], \quad (1.2)$$

are applied in the analogous electromagnetic transitions. The most favorable situations appear in light nuclei, where the approximation of free nucleons used for construction of the transition operators is commonly accepted. In other words, we treat the vector and axial currents on equal footing and we consider Eq.(1.1) to be as important for the axial current as Eq.(1.2) is important for the vector current.

The structure of the paper is as follows. In Sect.II, we consider the two-nucleon weak axial relativistic amplitudes of the  $\rho$ -,  $\omega$ -, and  $a_1$  ranges, derived from the Lagrangian [38] and we list the PCAC equations which the amplitudes satisfy. In Sect.III, we first define the WANECs as the difference of the relativistic exchange amplitude and of the first Born iteration of the nuclear equation of motion. Next we derive the nuclear PCAC that the WANECs should satisfy. Then we proceed to investigate the structure of the WANECs and present the resulting currents in the leading order in  $1/M$ .

In Sect. IV, we provide numerical estimates of the cross sections and of the strength of various parts of the space component of our WANECs for the weak deuteron disintegration by the low energy (anti)neutrinos and compare them with the calculations of Refs. [12, 75, 80, 81]. We discuss our results in Sect.V. Our notations and basic definitions are shortly presented in appendix A, and the structure of the weak axial  $\sigma$  meson exchange current is shortly discussed in appendix B.

## II. TWO-NUCLEON WEAK AXIAL MESON EXCHANGE AMPLITUDES OF THE $\rho$ , $a_1$ AND $\omega$ RANGES

We first write the weak axial amplitude for the  $i$ th nucleon ( $i = 1, 2$ )

$$J_{5\mu}^a(1, i) = -i \frac{g_A}{2} m_{a_1}^2 \Delta_{\mu\nu}^{a_1}(q_i) \tilde{\Gamma}_{5\nu}^a(i) - i f_\pi q_{i\mu} \Delta_F^\pi(q_i^2) \Gamma_i^{\pi a} \equiv \bar{u}(p'_i) \hat{J}_{5\mu}(1, i) \frac{\tau_i^a}{2} u(p_i). \quad (2.1)$$

Here  $q_i = p'_i - p_i$ , the vector-meson propagator is generally designed as

$$\Delta_{\mu\nu}^B(q) = \left( \delta_{\mu\nu} + \frac{q_\mu q_\nu}{m_B^2} \right) \Delta_F^B(q^2), \quad \Delta_F^B(q^2) = \frac{1}{m_B^2 + q^2}, \quad (2.2)$$

and the pseudovector and pseudoscalar vertices are defined as

$$\tilde{\Gamma}_{5\nu}^a(i) = \bar{u}(p'_i) \gamma_\nu \gamma_5 \tau_i^a u(p_i), \quad \Gamma_i^{\pi a} = i g \bar{u}(p'_i) \gamma_5 \tau_i^a u(p_i) \equiv \bar{u}(p'_i) \hat{O}_i^\pi \tau_i^a u(p_i). \quad (2.3)$$

The divergence of the amplitude (2.1) is

$$q_\mu J_{5\mu}^a(1, i) = i f_\pi m_\pi^2 \Delta_F^\pi(q_i^2) M^a(1, i). \quad (2.4)$$

Here the one–body pion absorption amplitude  $M^a(1, i)$  is defined as

$$M^a(1, i) = \Gamma_i^{\pi^a}. \quad (2.5)$$

The general structure of the two–nucleon weak axial amplitudes of our model is given in Fig. 1. We shall next consider  $\rho$ ,  $a_1$  and  $\omega$  exchanges. As in the pion exchange case [39, 40], we study first the relativistic exchange amplitudes.

### A. Two–nucleon weak axial exchange amplitudes of the $\rho$ , $a_1$ and $\omega$ meson range

Let us first write down the general form of the nucleon Born amplitude

$$J_{5\mu, B}^a \equiv J_{5\mu, B}^a(a_1) + J_{5\mu, B}^a(\pi) = -\bar{u}(p'_1) \left[ \hat{O}_{1(\nu)}^B(-q_2) S_F(P) \hat{J}_{5\mu}(1, q) \frac{1}{2}(a^+ - a^-) + \hat{J}_{5\mu}(1, q) \right. \\ \left. \times S_F(Q) \hat{O}_{1(\nu)}^B(-q_2) \frac{1}{2}(a^+ + a^-) \right] u(p_1) \Delta_{(\nu\eta)}^B(q_2) \bar{u}(p'_2) \hat{O}_{2(\eta)}^B(q_2) u(p_2) + (1 \leftrightarrow 2), \quad (2.6)$$

where it holds for various meson exchanges

$$B = \rho, \quad \hat{O}_{i\eta}^\rho(q_2) = -i \frac{g_\rho}{2} (\gamma_\eta - \frac{\kappa_\rho^V}{2M} \sigma_{\eta\delta} q_{2\delta})_i \equiv -i g_{\rho NN} \tilde{O}_{i\eta}^\rho(q_2), \quad (2.7)$$

$$B = \omega, \quad \hat{O}_{i\eta}^\omega(q_2) = -i \frac{g_\omega}{2} (\gamma_\eta - \frac{\kappa_\omega^S}{2M} \sigma_{\eta\delta} q_{2\delta})_i \equiv -i g_{\omega NN} \tilde{O}_{i\eta}^\omega(q_2), \quad \tau^n \rightarrow 1, \quad (2.8)$$

$$B = a_1, \quad \hat{O}_{i\eta}^{a_1} = -i g_\rho g_A (\gamma_\eta \gamma_5)_i \equiv -i g_{a_1 NN} \tilde{O}_{i\eta}^{a_1}, \quad (2.9)$$

$$(2.10)$$

and

$$a^\pm = \frac{1}{2} [\tau_1^a, \tau_1^n]_\pm \tau_2^n. \quad (2.11)$$

For the isovector meson exchange

$$a^+ = \tau_2^a, \quad a^- = -i(\vec{\tau}_1 \times \vec{\tau}_2)^a, \quad (2.12)$$

whereas for the isoscalar meson exchange

$$a^+ = \tau_1^a, \quad a^- = 0. \quad (2.13)$$

As it will become clear soon, the  $\rho$  and  $a_1$  exchanges should be considered in the chiral model [38] simultaneously.

Other weak axial exchange and pion absorption amplitudes can be derived from the operator amplitudes, constructed in Ref.[50] in conjunction with the Bethe–Salpeter equation, by sandwiching them between the Dirac spinors for the free nucleons. The weak axial exchange amplitudes of the  $\rho$  meson range are as follows. Besides the nucleon Born amplitude,  $J_{5\mu, \rho}^a$ , the only potential contact term is  $J_{5\mu, c\rho}^a(\pi)$ . The mesonic amplitudes belong to the non–potential ones and they are  $J_{5\mu, a_1\rho}^a(a_1)$  and  $J_{5\mu, a_1\rho}^a(\pi)$ . Considered together with the  $\rho$  meson exchange amplitudes, the  $a_1$  meson ones contain only the potential amplitudes, that are the nucleon Born terms  $J_{5\mu, a_1}^a$  and three contact terms  $J_{5\mu, c_i a_1}^a(\pi)$  ( $i=1,2,3$ ). It can be verified that separately, the exchange amplitudes  $J_{5\mu, \rho}^a(2)$  and  $J_{5\mu, a_1}^a(2)$ , defined as

$$J_{5\mu, \rho}^a(2) = J_{5\mu, \rho}^a + J_{5\mu, c\rho}^a(\pi) + J_{5\mu, a_1\rho}^a(a_1) + J_{5\mu, a_1\rho}^a(\pi), \quad (2.14)$$

and

$$J_{5\mu, a_1}^a(2) = J_{5\mu, a_1}^a + \sum_{i=1}^3 J_{5\mu, c_i a_1}^a(\pi), \quad (2.15)$$

respectively, do not satisfy the standard PCAC constraint.

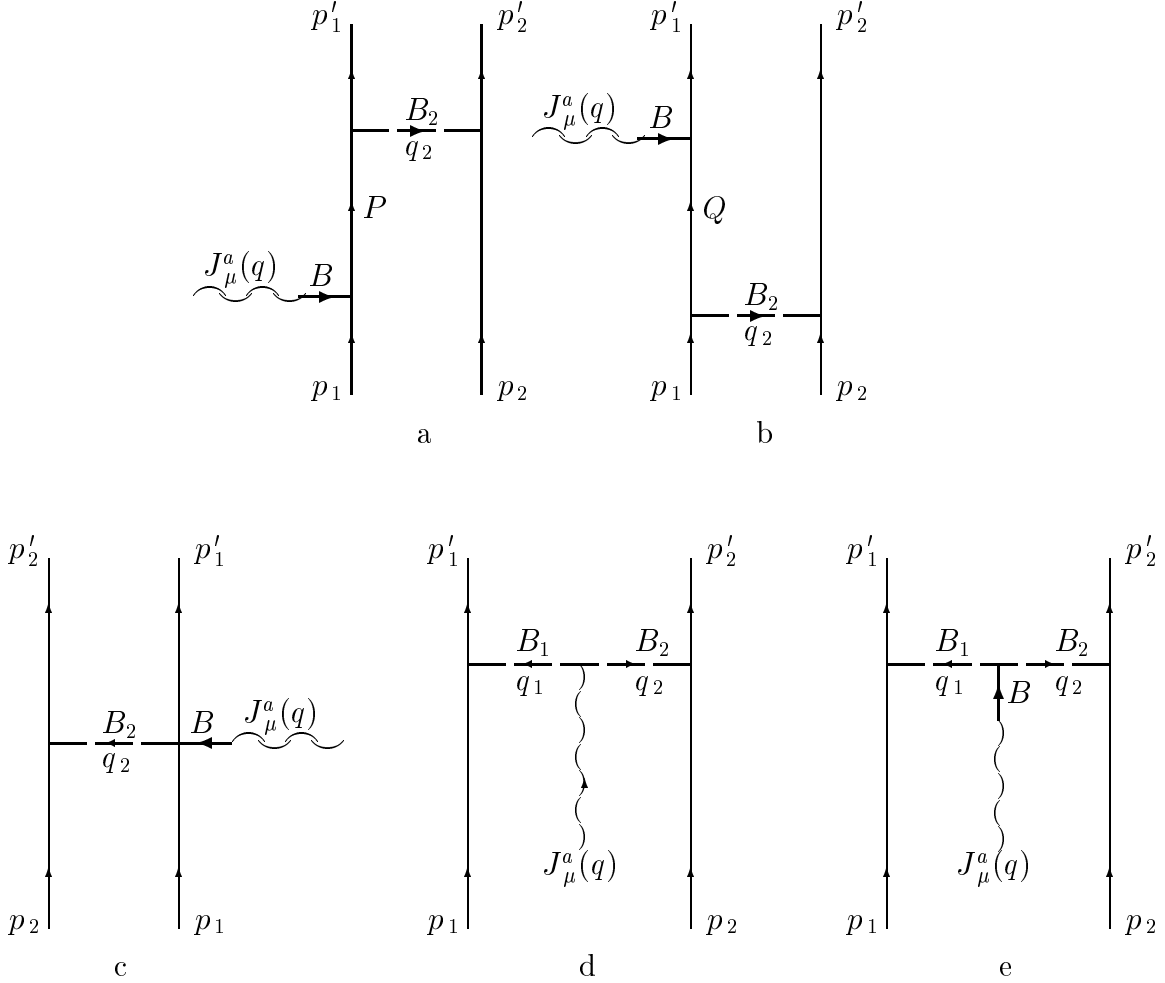


FIG. 1: The general structure of the two-nucleon weak axial amplitudes considered in this paper. The weak axial interaction is mediated by the meson  $B$  that is either  $\pi$  or  $a_1$  meson. The range of the amplitude is given by the meson  $B_2$  that is here  $\rho$ ,  $a_1$  or  $\omega$  meson; (a),(b) – the nucleon Born amplitude  $J_{5\mu, B_2}^a(B)$ ; (c) – a contact amplitude  $J_{5\mu, c B_2}^a(B)$ ; it is connected with the weak production amplitude of the  $B_2$  meson on the nucleon. Another type of the contact terms,  $J_{5\mu, B_1 B_2}^a$ , is given in (d), where the weak axial amplitude interacts directly with the mesons  $B_1$  and  $B_2$ . (e) – a mesonic amplitude  $J_{5\mu, B_1 B_2}^a(B)$ . The associated pion absorption amplitudes correspond to the graphs where the weak axial interaction is mediated by the pion, but with the weak interaction wavy line removed. There are three types of these amplitudes in our models:  $M_{B_2}^a$ ,  $M_{c B_2}^a$  and  $M_{B_1 B_2}^a$ .

However, using a derivation analogous to that of Sect. 3 of Ref. [50], one finds <sup>§</sup> that the sum of the amplitudes (2.14) and (2.15) satisfies the PCAC equation

$$q_\mu \left[ J_{5\mu,\rho}^a(2) + J_{5\mu,a_1}^a(2) \right] = if_\pi m_\pi^2 \Delta_F^\pi(q^2) \left[ M_\rho^a(2) + M_{a_1}^a(2) \right]. \quad (2.16)$$

The  $\omega$  meson exchange amplitudes contain only the potential amplitudes  $J_{5\mu,\omega}^a$  and  $J_{5\mu,c\omega}^a(\pi)$ . The divergence of the  $\omega$  meson exchange amplitude  $J_{5\mu,\omega}^a(2)$ , defined as

$$J_{5\mu,\omega}^a(2) = J_{5\mu,\omega}^a + J_{5\mu,c\omega}^a(\pi), \quad (2.17)$$

yields the PCAC equation

$$q_\mu J_{5\mu,\omega}^a(2) = if_\pi m_\pi^2 \Delta_F^\pi(q^2) M_\omega^a(2). \quad (2.18)$$

Using the results obtained in [50], one can derive the two-nucleon weak axial and pion absorption amplitudes from the Lagrangian [51] in the same manner. We mention only that the  $\rho$  and  $a_1$  exchange amplitudes satisfy the PCAC separately and that the model dependence should be expected at higher energies, because it is of the short range nature. In the next section, starting from the obtained two-nucleon weak axial exchange amplitudes, we derive the WANECs of the heavy meson range.

### III. WEAK AXIAL NUCLEAR EXCHANGE CURRENTS

We define the WANEC of the range B as

$$j_{5\mu,B}^a(2) = J_{5\mu,B}^a(2) - t_{5\mu,B}^{a, FBI}, \quad (3.1)$$

where the two-nucleon amplitudes  $J_{5\mu,B}^a(2)$  are derived in the previous section, and  $t_{5\mu,B}^{a, FBI}$  is the first Born iteration of the one-nucleon current contribution to the two-nucleon scattering amplitude, satisfying the Lippmann-Schwinger equation [58],

$$\begin{aligned} t_{5\mu,B}^{a, FBI} = & V_B(\vec{p}'_1, \vec{p}'_2; \vec{P}, \vec{p}_2) \frac{1}{P_0 - E(\vec{P}) + i\varepsilon} j_{5\mu}^a(1, \vec{P}, \vec{p}_1) \\ & + j_{5\mu}^a(1, \vec{p}'_1, \vec{Q}) \frac{1}{Q_0 - E(\vec{Q}) + i\varepsilon} V_B(\vec{Q}, \vec{p}'_2; \vec{p}_1, \vec{p}_2) + (1 \leftrightarrow 2), \end{aligned} \quad (3.2)$$

where  $\vec{P} = \vec{p}'_1 + \vec{q}_2 = \vec{p}_1 + \vec{q}$  and  $\vec{Q} = \vec{p}_1 - \vec{q}_2 = \vec{p}'_1 - \vec{q}$ , as it is seen from Fig. 2. Further,  $V_B$  is the one-boson exchange nuclear potential and

$$j_{5\mu}^a(1, \vec{p}', \vec{p}) = \bar{u}(p') \hat{J}_{5\mu}^a(1, 1) u(p), \quad (3.3)$$

is the weak axial nuclear one-nucleon current in the momentum space. It is the non-relativistic reduction of the one-nucleon amplitude  $J_{5\mu}^a(1, 1)$ , given in Eq. (2.1). In the nucleon kinematics,  $\vec{q}_1 = \vec{p}'_1 - \vec{p}_1$  and  $q_{10} = E(\vec{p}'_1) - E(\vec{p}_1)$ . The amplitude  $J_{5\mu,B}^a(2)$  contains the nucleon Born terms, graphically presented in Figs. 1(a) and 1(b). For them, however, the four-momentum conservation takes place. Next we derive the continuity equation for the WANEC.

<sup>§</sup> For more details see also Sect. III of Ref. [82].

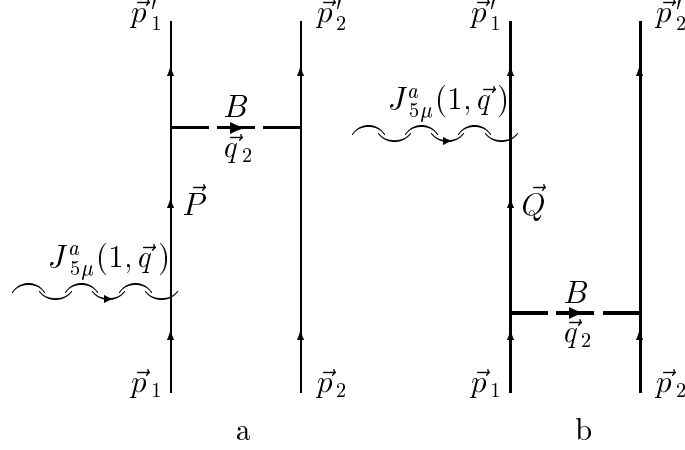


FIG. 2: The kinematics of the first Born iteration. The nucleon line in the intermediate state is on-shell.

### A. The PCAC equation for the WANEC

In order to derive the nuclear PCAC for the current  $j_{5\mu,B}^a(2)$ , we should know the continuity equation for the first Born iteration  $t_{5\mu,B}^{a,FBI}$ . This equation is

$$\begin{aligned}
q_\mu t_{5\mu,B}^{a,FBI} &= if_\pi m_\pi^2 \Delta_F^\pi(\vec{q}^2) \left[ V_B(\vec{p}'_1, \vec{p}'_2; \vec{P}, \vec{p}_2) \frac{1}{P_0 - E(\vec{P}) + i\varepsilon} m^a(1, \vec{P}, \vec{p}_1) \right. \\
&\quad \left. + m^a(1, \vec{p}'_1, \vec{Q}) \frac{1}{Q_0 - E(\vec{Q}) + i\varepsilon} V_B(\vec{Q}, \vec{p}'_2; \vec{p}_1, \vec{p}_2) \right] - [V_B, \rho_5^a(1)] \\
&\quad + (1 \leftrightarrow 2),
\end{aligned} \tag{3.4}$$

where

$$[V_B, \rho_5^a(1)] \equiv V_B(\vec{p}'_1, \vec{p}'_2; \vec{P}, \vec{p}_2) \rho_5^a(1, \vec{P}, \vec{p}_1) - \rho_5^a(1, \vec{p}'_1, \vec{Q}) V_B(\vec{Q}, \vec{p}'_2; \vec{p}_1, \vec{p}_2). \tag{3.5}$$

It follows from Eqs. (2.16) and (2.18) that the divergence of the amplitude  $J_{5\mu,B}^a(2)$  can be written as

$$q_\mu J_{5\mu,B}^a(2) = if_\pi m_\pi^2 \Delta_F^\pi(\vec{q}^2) M_B^a(2). \tag{3.6}$$

Using Eqs. (3.4) and (3.6), we derive the PCAC for the WANEC, defined in Eq. (3.1)

$$q_\mu j_{5\mu,B}^a(2) = if_\pi m_\pi^2 \Delta_F^\pi(\vec{q}^2) m_B^a(2) + ([V_B, \rho_5^a(1)] + (1 \leftrightarrow 2)), \tag{3.7}$$

where

$$m_B^a(2) = M_B^a(2) - m_B^{a,FBI}, \tag{3.8}$$

and the first Born iteration of the one-nucleon pion absorption amplitude is

$$\begin{aligned}
m_B^{a,FBI} &= V_B(\vec{p}'_1, \vec{p}'_2; \vec{P}, \vec{p}_2) \frac{1}{P_0 - E(\vec{P}) + i\varepsilon} m^a(1, \vec{P}, \vec{p}_1) \\
&\quad + m^a(1, \vec{p}'_1, \vec{Q}) \frac{1}{Q_0 - E(\vec{Q}) + i\varepsilon} V_B(\vec{Q}, \vec{p}'_2; \vec{p}_1, \vec{p}_2) + (1 \leftrightarrow 2).
\end{aligned} \tag{3.9}$$

We shall call the amplitude  $m_B^a(2)$  the nuclear two–nucleon pion absorption amplitude of the range B. It is seen from Eq. (3.8) that it is defined in the same way as the WANEC in Eq. (3.1).

We now pass to investigate the structure of the WANECs.

## B. The structure of the WANECs

As it is seen from Eq.(3.1), the structure of the WANECs differs from the structure of the two–nucleon weak axial exchange amplitudes studied in the previous section. In the case of the Schrödinger equation, the positive frequency part of the nucleon Born term and the first Born iteration differ and this difference provides a contribution to the WANECs. Here we shall calculate this difference. For this purpose, we split the nucleon propagator  $S_F$  into the positive,  $S_F^{(+)}$ , and negative,  $S_F^{(-)}$ , frequency parts (see App. A). Then the positive frequency part  $J_{5\mu,B}^{a(+)}$  of the nucleon Born term  $J_{5\mu,B}^a$ , Eq. (2.6), can be cast into the form

$$\begin{aligned} J_{5\mu,B}^{a(+)} &= \mathcal{V}_B(p'_1, p'_2; P, p_2) \frac{1}{P_0 - E(\vec{P})} \tilde{J}_{5\mu}(1, P, p_1) \frac{1}{2}(a^+ - a^-) \\ &\quad + \tilde{J}_{5\mu}(1, p'_1, Q) \frac{1}{Q_0 - E(\vec{Q})} \mathcal{V}_B(Q, p'_2; p_1, p_2) \frac{1}{2}(a^+ + a^-) + (1 \leftrightarrow 2), \end{aligned} \quad (3.10)$$

where the quasipotential  $\mathcal{V}_B$  is defined as

$$\mathcal{V}_B(p'_1, p'_2; p_1, p_2) = g_{BNN}^2 \bar{u}(p'_1) \tilde{\mathcal{O}}_{(\lambda)}^B(-q_2) u(p_1) \Delta_{(\lambda n)}^B(q_2) \bar{u}(p'_2) \tilde{\mathcal{O}}_{(n)}^B(q_2) u(p_2), \quad (3.11)$$

and  $\tilde{J}_{5\mu}$  is the amplitude Eq.(2.1) without  $\tau^a/2$ . For the amplitude  $t_{5\mu,B}^{a,FBI}$ , Eq. (3.2), one can write in a similar way

$$\begin{aligned} t_{5\mu,B}^{a,FBI} &= \tilde{V}_B(\vec{p}'_1, \vec{p}'_2; \vec{P}, \vec{p}_2) \frac{1}{P_0 - E(\vec{P}) + i\varepsilon} \tilde{j}_{5\mu}(1, \vec{P}, \vec{p}_1) \frac{1}{2}(a^+ - a^-) \\ &\quad + \tilde{j}_{5\mu}(1, \vec{p}'_1, \vec{Q}) \frac{1}{Q_0 - E(\vec{Q}) + i\varepsilon} \tilde{V}_B(\vec{Q}, \vec{p}'_2; \vec{p}_1, \vec{p}_2) \frac{1}{2}(a^+ + a^-) + (1 \leftrightarrow 2) \end{aligned} \quad (3.12)$$

where  $\tilde{V}_B$  and  $\tilde{j}_{5\mu}$  correspond to  $V_B$  and  $j_{5\mu}^a$ , respectively, but without the isospin dependence. Using the definition Eq. (3.1) and Eqs. (3.10) and (3.12), we can calculate the contribution to the WANEC arising from the difference of the positive frequency nucleon Born terms and the first Born iteration

$$\begin{aligned} \Delta J_{5\mu,B}^{a(+)} &= J_{5\mu,B}^{a(+)} - t_{5\mu,B}^{a,FBI} \\ &= \frac{1}{P_0 - E(\vec{P}) + i\varepsilon} D_{\mu,B}(P) \frac{1}{2}(a^+ - a^-) + \frac{1}{Q_0 - E(\vec{Q}) + i\varepsilon} D_{\mu,B}(Q) \frac{1}{2}(a^+ + a^-) \\ &\quad + (1 \leftrightarrow 2), \end{aligned} \quad (3.13)$$

$$D_{\mu,B}(P) = \mathcal{V}_B(p'_1, p'_2; P, p_2) \tilde{J}_{5\mu}(1, P, p_1) - \tilde{V}_B(\vec{p}'_1, \vec{p}'_2; \vec{P}, \vec{p}_2) \tilde{j}_{5\mu}(1, \vec{P}, \vec{p}_1), \quad (3.14)$$

$$D_{\mu,B}(Q) = \tilde{J}_{5\mu}(1, p'_1, Q) \mathcal{V}_B(Q, p'_2; p_1, p_2) - \tilde{j}_{5\mu}(1, \vec{p}'_1, \vec{Q}) \tilde{V}_B(\vec{Q}, \vec{p}'_2; \vec{p}_1, \vec{p}_2). \quad (3.15)$$

Checking the structure of the currents and potentials, one can see that the contributions to  $\Delta J_{5\mu,B}^{a(+)}$  can arise from the difference in the dependence on the energy transfer of the BNN

vertices, of the currents, and of the B-meson propagators. We shall call them the vertex, external and retardation currents, respectively. They satisfy the equation,

$$\Delta j_{5\mu, B}^{a(+)} = j_{5\mu, B}^a(vert) + j_{5\mu, B}^a(ext) + j_{5\mu, B}^a(ret). \quad (3.16)$$

Besides these corrections, one obtains the whole set of terms by the standard non-relativistic reduction of the amplitudes  $J_{5\mu, B}^a(2)$  up to the desired order in  $1/M$ .

### C. Results

In this section, we present the resulting WANECS.

#### 1. Vertex currents

As it is seen from Eqs. (2.7) and (2.8), the  $\rho$ - and  $\omega$  exchanges can contribute into the vertex current  $j_{5\mu, B}^a(vert)$ . This contribution can be calculated by expanding in the BNN vertex of the pseudopotential  $\mathcal{V}_B$  around  $P_0 = E(\vec{P})$  and  $Q_0 = E(\vec{Q})$ . Then one obtains

$$\begin{aligned} \mathcal{V}_B(p'_1, p'_2; P, p_2) &= \tilde{V}_B(\vec{p}'_1, \vec{p}'_2; \vec{P}, \vec{p}_2) + ig_{BNN}^2 \frac{\kappa^B}{2M} [P_0 - E(\vec{P})] \\ &\times \bar{u}(p'_1) \sigma_{j4} u(P) \Delta_{j\eta}^B(q_2) \bar{u}(p'_2) \tilde{\mathcal{O}}_\eta^{B, st}(q_2) u(p_2), \end{aligned} \quad (3.17)$$

and

$$\begin{aligned} \mathcal{V}_B(Q, p'_2; p_1, p_2) &= \tilde{V}_B(\vec{Q}, \vec{p}'_2; \vec{p}_1, \vec{p}_2) + ig_{BNN}^2 \frac{\kappa^B}{2M} [E(\vec{Q}) - Q_0] \\ &\times \bar{u}(Q) \sigma_{j4} u(p_1) \Delta_{j\eta}^B(q_2) \bar{u}(p'_2) \tilde{\mathcal{O}}_\eta^{B, st}(q_2) u(p_2). \end{aligned} \quad (3.18)$$

Substituting the expansions Eqs. (3.17) and (3.18) into Eqs. (3.13)–(3.15) we obtain

$$\begin{aligned} j_{5\mu, B}^a(vert) &= ig_{BNN}^2 \frac{\kappa^B}{2M} \left[ \bar{u}(p'_1) \sigma_{j4} u(P) \tilde{j}_{5\mu}(1, \vec{P}, \vec{p}_1) \frac{1}{2} (a^+ - a^-) - \tilde{j}_{5\mu}(1, \vec{p}'_1, \vec{Q}) \bar{u}(Q) \sigma_{j4} u(p_1) \right. \\ &\left. \times \frac{1}{2} (a^+ + a^-) \right] \Delta_{j\eta}^B(q_2) \bar{u}(p'_2) \tilde{\mathcal{O}}_\eta^{B, st}(q_2) u(p_2) + (1 \leftrightarrow 2). \end{aligned} \quad (3.19)$$

Performing the non-relativistic reduction and preserving only the part  $\sim (1 + \kappa^B)$ , the space part of Eq. (3.19) reduces to

$$\begin{aligned} \vec{j}_{5, B}^a(vert) &= \frac{g_{BNN}^2}{(2M)^3} \kappa^B (1 + \kappa^B) \left\langle g_A F_A \left\{ a^+ \left[ \vec{q} \times (\vec{\sigma}_2 \times \vec{q}_2) + i \vec{\sigma}_1 \times (\vec{P}_1 \times (\vec{\sigma}_2 \times \vec{q}_2)) \right] \right. \right. \\ &\left. \left. + i a^- \left[ i \vec{P}_1 \times (\vec{\sigma}_2 \times \vec{q}_2) - \vec{\sigma}_1 \times (\vec{q} \times (\vec{\sigma}_2 \times \vec{q}_2)) \right] \right\} \right. \\ &\left. + \frac{g_P}{m_l} \frac{\vec{q}}{2M} \left\{ i a^+ \left[ \vec{q} \cdot \vec{\sigma}_1 \times (\vec{P}_1 \times (\vec{\sigma}_2 \times \vec{q}_2)) \right] + i a^- \left[ i \vec{q} \cdot \vec{P}_1 \times (\vec{\sigma}_2 \times \vec{q}_2) \right. \right. \right. \\ &\left. \left. \left. - \vec{q} \cdot \vec{\sigma}_1 \times (\vec{q} \times (\vec{\sigma}_2 \times \vec{q}_2)) \right] \right\} \right\rangle \Delta_F^B(\vec{q}_2^2) + (1 \leftrightarrow 2), \end{aligned} \quad (3.20)$$

where  $\vec{P}_i = \vec{p}'_i + \vec{p}_i$ ,  $g_P(\vec{q}^2)/m_l = 2gf_\pi\Delta_F^\pi(\vec{q}^2)$ , and  $m_l$  is the lepton mass. This current is important for the  $\rho$  meson exchange, since  $\kappa^B = \kappa_\rho^V \approx 6.6$ .

Analogous calculations for the time component  $j_{50,B}^a(vert)$  show that in comparison with the space component, Eq. (3.20), it is by one order in  $1/M$  suppressed,

$$j_{50,B}^a(vert) \approx \mathcal{O}(1/M^4). \quad (3.21)$$

According to the definition of the exchange currents in Refs. [25, 45], only the negative frequency part of the nucleon Born terms contributes. So the vertex currents are absent in [45]. It means that the currents [45] are suitable for calculations with the nuclear wave functions that are solution of the equation of motion, providing the first Born iteration that cancels exactly the positive frequency part of the nucleon Born currents, in order to avoid the double counting. In the pion exchange current the analogous vertex current of our approach is again of the nominal order  $\mathcal{O}(M^{-3})$  [39, 62], if the chiral model with the pseudovector  $\pi NN$  coupling is used. In the chiral model with the pseudoscalar  $\pi NN$  coupling, the vertex current is absent, but the sum of the negative frequency part of the nucleon Born term and of the PCAC constraint term yields the same result [18, 40, 62]. Without the vertex current included, the pion exchange current [45] is  $\approx \mathcal{O}(M^{-5})$ .

## 2. External exchange currents

These currents arise from the  $q_0$  dependence of the amplitudes  $\tilde{J}_{5\mu}$  in Eqs. (3.14) and (3.15). One obtains [82]

$$\begin{aligned} \vec{j}_{5,B}^a(ext) &\approx g_A \frac{\vec{q}}{4M} \Delta_F^{a1}(q^2) \left\{ -a^+ [\tilde{V}_B^{(1)}(\vec{q}_2)(\vec{\sigma}_1 \cdot (\vec{P}_1 + \vec{q}_2)) - (\vec{\sigma}_1 \cdot (\vec{P}_1 - \vec{q}_2))\tilde{V}_B^{(1)}(\vec{q}_2)] \right. \\ &\quad \left. + a^- [\tilde{V}_B^{(1)}(\vec{q}_2)(\vec{\sigma}_1 \cdot (\vec{P}_1 + \vec{q}_2)) + (\vec{\sigma}_1 \cdot (\vec{P}_1 - \vec{q}_2))\tilde{V}_B^{(1)}(\vec{q}_2)] \right\} + (1 \leftrightarrow 2) \quad (3.22) \\ j_{50,B}^a(ext) &\approx \frac{g_A}{2} [\Delta_F^{a1}(q^2) - \Delta_F^\pi(q^2)] \left\{ a^+ [\tilde{V}_B^{(1)}(\vec{q}_2)(\vec{\sigma}_1 \cdot \vec{q}) - (\vec{\sigma}_1 \cdot \vec{q})\tilde{V}_B^{(1)}(\vec{q}_2)] \right. \\ &\quad \left. - a^- [\tilde{V}_B^{(1)}(\vec{q}_2)(\vec{\sigma}_1 \cdot \vec{q}) + (\vec{\sigma}_1 \cdot \vec{q})\tilde{V}_B^{(1)}(\vec{q}_2)] \right\} + (1 \leftrightarrow 2). \quad (3.23) \end{aligned}$$

Here  $\tilde{V}_B^{(1)}$  is the leading order term in the B-meson exchange potential  $\tilde{V}_B$ . In deriving these equations, we neglected terms  $\sim [\Delta_F^B(q^2)]^2$ .

## 3. Pair term retardation

This contribution arises from the pair terms due to the all meson exchanges and it appears from the difference between the energy dependence in the propagator of the pseudopotential and the potential [58]. The final result for the retardation currents is [82]

$$\begin{aligned} j_{5\mu,B}^a(ret) &= \frac{1}{4M} \left\langle \left\{ (1 + \nu)(\vec{P}_2 \cdot \vec{q}_2) + (1 - \nu)[(\vec{P}_1 + \vec{q}) \cdot \vec{q}_2] \right\} \tilde{V}_B^{(1)}(\vec{q}_2) \tilde{j}_{5\mu}(1, \vec{P}, \vec{p}_1) \right. \\ &\quad \times \frac{1}{2} (a^+ - a^-) - \left\{ (1 + \nu)(\vec{P}_2 \cdot \vec{q}_2) + (1 - \nu)[(\vec{P}_1 - \vec{q}) \cdot \vec{q}_2] \right\} \tilde{j}_{5\mu}(1, \vec{p}'_1, \vec{Q}) \\ &\quad \left. \times \tilde{V}_B^{(1)}(\vec{q}_2) \frac{1}{2} (a^+ + a^-) \right\rangle \Delta_F^B(\vec{q}_2^2) + (1 \leftrightarrow 2). \quad (3.24) \end{aligned}$$

Here  $\nu$  is a parameter of a unitary transformation (cf. [83]).

#### 4. Negative frequency part of the nucleon Born terms

This contribution arises from the nucleon Born currents  $J_{5\mu, B}^a$ , Eq. (2.6), by the change  $S_F \rightarrow S_F^{(-)}$ . We consider first the  $B=\rho$  and  $\omega$  meson exchanges. After the non-relativistic reduction, we obtain for the negative frequency terms of the  $\rho$ - and  $\omega$  ranges

$$\begin{aligned}
\vec{j}_{5, B}^{a(-)} &= \frac{g_{BNN}^2}{(2M)^3} (1 + \kappa^B) \left\langle a^+ \left\{ g_A F_A [(\vec{\sigma}_1 \cdot \vec{q}_2) \vec{q} + \vec{q}_2 \times ((\vec{\sigma}_1 + \vec{\sigma}_2) \times \vec{q}_2) \right. \right. \\
&\quad \left. \left. + i\vec{P}_1 \times (\vec{\sigma}_1 \times (\vec{\sigma}_2 \times \vec{q}_2)) - i(\vec{P}_1 \times \vec{q}_2) \right] - 2M \frac{g_P(q^2)}{m_l} (\vec{\sigma}_1 \cdot \vec{q}_2) \vec{q} \right\} \\
&\quad - a^- \left\{ g_A F_A \left[ i(\vec{\sigma}_1 \cdot \vec{\sigma}_2 \times \vec{q}_2) \vec{q} + \vec{P}_1 \times (\vec{\sigma}_2 \times \vec{q}_2) + i\vec{q}_2 \times (\vec{\sigma}_1 \times (\vec{\sigma}_2 \times \vec{q}_2)) \right. \right. \\
&\quad \left. \left. + \vec{P}_1 \times (\vec{\sigma}_1 \times \vec{q}_2) \right] - 2iM \frac{g_P(q^2)}{m_l} (\vec{\sigma}_1 \cdot \vec{\sigma}_2 \times \vec{q}_2) \vec{q} \right\} \right\rangle \Delta_F^B(\vec{q}_2^2) \\
&\quad + \frac{g_{BNN}^2}{(2M)^3} \left\langle a^+ g_A F_A \left[ -i(\vec{q}_2 \times \vec{P}_2) + \vec{P}_1 \times (\vec{\sigma}_1 \times \vec{P}_2) \right] - a^- \left\{ g_A F_A \left[ (\vec{\sigma}_1 \cdot \vec{P}_2) \vec{q} \right. \right. \right. \\
&\quad \left. \left. - i(\vec{P}_1 \times \vec{P}_2) + \vec{q}_2 \times (\vec{\sigma}_1 \times \vec{P}_2) \right] - 2M \frac{g_P(q^2)}{m_l} (\vec{\sigma}_1 \cdot \vec{P}_2) \vec{q} \right\} \right\rangle \Delta_F^B(\vec{q}_2^2) + (1 \leftrightarrow 2) \quad (3.25) \\
j_{50, B}^{a(-)} &= \frac{g_{BNN}^2}{(2M)^2} \left\langle (1 + \kappa^B) \left\{ -a^+ \left[ g_A F_A i(\vec{\sigma}_1 \cdot \vec{\sigma}_2 \times \vec{q}_2) + \frac{g_P(q^2)}{m_l} q_0 (\vec{\sigma}_1 \cdot \vec{q}_2) \right] \right. \right. \\
&\quad \left. \left. + a^- \left[ g_A F_A (\vec{\sigma}_1 \cdot \vec{q}_2) + i \frac{g_P(q^2)}{m_l} q_0 (\vec{\sigma}_1 \cdot \vec{\sigma}_2 \times \vec{q}_2) \right] \right\} - a^+ g_A F_A (\vec{\sigma}_1 \cdot \vec{P}_2) \right. \\
&\quad \left. + a^- \frac{g_P(q^2)}{m_l} q_0 (\vec{\sigma}_1 \cdot \vec{P}_2) \right\rangle \Delta_F^B(\vec{q}_2^2) + (1 \leftrightarrow 2). \quad (3.26)
\end{aligned}$$

Comparing our current of Eq. (3.25) with the current  $\vec{A}_\pm(V)$  of Ref. [45] we can see a difference in the term of the form  $\vec{\sigma}_1 \vec{q}_2^2$ . Spurious factor 1/4 appears in [45] due to the use of  $S_F^{(-)}(p) = (i\vec{\gamma} \cdot \vec{p} - M + \gamma_4 E(\vec{p}^2))/4M^2$ , and approximating  $E = M$ , when calculating the contribution from the  $\gamma_4 \gamma_4$  part of the vector exchange. The same is true also for the scalar-isoscalar exchange. The correct result is obtained by making use of  $E = M + \vec{p}^2/2M$ . Summing up the currents  $\vec{j}_{5, B}^a(vert)$ , Eq. (3.20), and  $\vec{j}_{5, B}^{a(-)}$ , Eq. (3.25) for  $B = \rho$ , and keeping only the terms  $\sim (1 + \kappa_\rho^V)$ , we arrive at the nuclear potential term of the  $\rho$  range<sup>¶</sup>

$$\begin{aligned}
\vec{j}_{5, \rho}^a(pot) &= \left( \frac{g_\rho}{2} \right)^2 \frac{(1 + \kappa_\rho^V)^2}{(2M)^3} g_A F_A \left\{ \tau_2^a \left[ \vec{q} \times (\vec{\sigma}_2 \times \vec{q}_2) + i\vec{\sigma}_1 \times (\vec{P}_1 \times (\vec{\sigma}_2 \times \vec{q}_2)) \right] \right. \\
&\quad \left. + (\vec{\tau}_1 \times \vec{\tau}_2)^a \left[ i\vec{P}_1 \times (\vec{\sigma}_2 \times \vec{q}_2) - \vec{\sigma}_1 \times (\vec{q} \times (\vec{\sigma}_2 \times \vec{q}_2)) \right] \right\} \Delta_F^\rho(\vec{q}_2^2) \\
&\quad - \left( \frac{g_\rho}{2} \right)^2 \frac{(1 + \kappa_\rho^V)}{(2M)^2} \frac{g_P(\vec{q}^2)}{m_l} \left[ \tau_2^a (\vec{\sigma}_1 \cdot \vec{q}_2) - (\vec{\tau}_1 \times \vec{\tau}_2)^a (\vec{\sigma}_1 \cdot \vec{\sigma}_2 \times \vec{q}_2) \right] \vec{q} \Delta_F^\rho(\vec{q}_2^2) \\
&\quad + (1 \leftrightarrow 2), \quad (3.27)
\end{aligned}$$

<sup>¶</sup> Here we follow the nomenclature of Ref. [62].

$$\begin{aligned}
j_{50,\rho}^a(\text{pot}) &= - \left( \frac{g_\rho}{2} \right)^2 \frac{(1 + \kappa_\rho^V)}{(2M)^2} \{ i g_A F_A [\tau_2^a (\vec{\sigma}_1 \cdot \vec{\sigma}_2 \times \vec{q}_2) + (\vec{\tau}_1 \times \vec{\tau}_2)^a (\vec{\sigma}_1 \cdot \vec{q}_2)] \\
&\quad + \frac{g_P(q^2)}{m_l} q_0 [\tau_2^a (\vec{\sigma}_1 \cdot \vec{q}_2) - (\vec{\tau}_1 \times \vec{\tau}_2)^a (\vec{\sigma}_1 \cdot \vec{\sigma}_2 \times \vec{q}_2)] \} \Delta_F^\rho(\vec{q}_2^2) \\
&\quad + (1 \leftrightarrow 2). \tag{3.28}
\end{aligned}$$

The part of our current  $j_{50,\rho}^a(\text{pot})$ , Eq. (3.28), that is  $\sim g_A$ , is in agreement with the current  $J_{50}^{(2)a}(v\text{-pair})$ , Eq. (38a), derived by Towner [26]. On the other hand, the part of our current  $\vec{j}_{5,\rho}^a(\text{pot})$ , Eq. (3.27), that is  $\sim g_A$ , differs from the  $\rho$  meson pair term, used by Schiavilla *et al.* [44] and also in Ref. [12].

Since  $\kappa_S \approx -0.12$ , we keep only the negative frequency Born term contribution into the omega meson potential term,

$$\begin{aligned}
\vec{j}_{5,\omega}^a(\text{pair}) &= \left( \frac{g_\omega}{2} \right)^2 \frac{1}{(2M)^3} \tau_1^a \left\langle g_A F_A \left\{ \vec{P}_1 \times (\vec{\sigma}_1 \times \vec{P}_2) - i(\vec{q}_2 \times \vec{P}_2) + (1 + \kappa_S) [\vec{q}(\vec{\sigma}_1 \cdot \vec{q}_2) \right. \right. \\
&\quad \left. \left. - i(\vec{P}_1 \times \vec{q}_2) + \vec{q}_2 \times ((\vec{\sigma}_1 + \vec{\sigma}_2) \times \vec{q}_2) + i\vec{P}_1 \times (\vec{\sigma}_1 \times (\vec{\sigma}_2 \times \vec{q}_2))] \right\} \right. \\
&\quad \left. - \frac{2M g_P}{m_l} (1 + \kappa_S) \vec{q}(\vec{\sigma}_1 \cdot \vec{q}_2) \right\rangle \Delta_F^\omega(\vec{q}_2^2) + (1 \leftrightarrow 2). \tag{3.29}
\end{aligned}$$

$$\begin{aligned}
j_{50,\omega}^a(\text{pair}) &= - \left( \frac{g_\omega}{2} \right)^2 \frac{1}{(2M)^2} \tau_1^a \left\{ g_A F_A [(\vec{\sigma}_1 \cdot \vec{P}_2) + i(1 + \kappa_S)(\vec{\sigma}_1 \cdot \vec{\sigma}_2 \times \vec{q}_2)] \right. \\
&\quad \left. + \frac{g_P}{m_l} q_0 (1 + \kappa_S)(\vec{\sigma}_1 \cdot \vec{q}_2) \right\} \Delta_F^\omega(\vec{q}_2^2) + (1 \leftrightarrow 2). \tag{3.30}
\end{aligned}$$

In this case, the potential and pair terms coincide. Analogous calculations for the  $a_1$  meson exchange yield the pair term that can be found in Ref. [82]. The currents studied so far are derived from the nucleon Born term amplitudes. We now present shortly the currents that have the origin in other amplitudes of the section II A.

### 5. Potential contact WANECS

Here we have the currents  $j_{5\mu,c\rho}^a(\pi)$ ,  $j_{5\mu,c_i a_1}^a(\pi)$ ,  $i=1,2,3$ , and  $j_{5\mu,c\omega}^a(\pi)$ , obtained by the non-relativistic reduction of the pion production amplitudes, entering the weak amplitudes  $J_{5\mu,c\rho}^a(\pi)$ ,  $J_{5\mu,c_i a_1}^a(\pi)$ ,  $i=1,2,3$ , and  $J_{5\mu,c\omega}^a(\pi)$ , respectively. The explicit results for the currents can be found in [82].

### 6. Non-potential WANECS

In the considered model, there are two non-potential currents,  $j_{5\mu,a_1\rho}^a(a_1)$  and  $j_{5\mu,a_1\rho}^a(\pi)$ , related to the mesonic amplitudes  $J_{5\mu,a_1\rho}^a(a_1)$  and  $J_{5\mu,a_1\rho}^a(\pi)$ , respectively [82]. They are of the  $\rho$  meson range. In the next section, we shall use the space component of the current  $j_{5\mu,a_1\rho}^a(a_1)$  in the numerical estimates of the cross sections. It reads

$$\begin{aligned}
\vec{j}_{5,a_1\rho}^a(a_1) &= \frac{1 + \kappa_\rho^V}{2M} \left( \frac{g_\rho}{2} \right)^2 g_A F_A(q^2) (\vec{\tau}_1 \times \vec{\tau}_2)^a \Delta_F^{a_1}(\vec{q}_1^2) [2(\vec{\sigma}_2 \cdot \vec{q}_1 \times \vec{q}_2) \vec{\sigma}_1 \\
&\quad + (\vec{\sigma}_1 \cdot \vec{q}) (\vec{\sigma}_2 \times \vec{q}_2) + (\vec{q}_2 \cdot \vec{\sigma}_1 \times \vec{\sigma}_2) \vec{q}_1] \Delta_F^\rho(\vec{q}_2^2) + (1 \leftrightarrow 2). \tag{3.31}
\end{aligned}$$

We have completed the construction of the heavy meson WANECS of our models. In the next section, we apply the leading terms of our currents in calculations of the cross sections for the weak deuteron disintegration by the low energy (anti)neutrinos.

#### IV. NUMERICAL RESULTS

We now calculate the cross sections for the reactions of the weak deuteron disintegration by low energy (anti)neutrinos,

$$\nu_x + d \longrightarrow \nu'_x + n + p, \quad (4.1)$$

$$\bar{\nu}_x + d \longrightarrow \bar{\nu}'_x + n + p, \quad (4.2)$$

$$\nu_e + d \longrightarrow e^- + p + p, \quad (4.3)$$

$$\bar{\nu}_e + d \longrightarrow e^+ + n + n, \quad (4.4)$$

where  $\nu_x$   $\bar{\nu}_x$  refers to any active flavor of the (anti)neutrino. The reactions (4.1) and (4.3) are important for studying the solar neutrino oscillations, whereas the reactions (4.2) and (4.4) occur in experiments with reactor antineutrino beams. The precise knowledge of the cross sections of the  $\nu d$  reactions is needed [84] for the calculations of the response functions of the SNO detector [85–88]. The total active ( $\nu_x$ )  ${}^8\text{Be}$  solar neutrino flux  $5.21 \pm 0.27$  (stat.)  $\pm 0.38$  (syst.)  $\times 10^6$   $\text{cm}^2 \text{s}^{-1}$  was found in agreement with the standard solar models prediction.

Theoretical studies of the reactions (4.1)-(4.4), including exchange currents, were accomplished in the SNPA in Refs. [12, 43, 80], and in the EFT's in Refs. [73–75]. The calculations [80, 81], accomplished within the SNPA, generally differ between themselves at the threshold energies by 5%-10% [75]. In our opinion, this provides a good motivation to make independent calculations. Before presenting our numerical results, we introduce necessary formalism and input data.

##### A. Formalism

Making use of the technique, developed in Refs. [89, 90], one obtains the following generic equation for the cross sections

$$\begin{aligned} \sigma = & \frac{1}{6\pi^2} M_r G_W^2 \int_{-1}^{+1} dx \int_0^{k'_{max}} dk' \kappa_0 k'^2 \left\{ \sum_{\lambda j_f, J \geq 0} [j_0 j_0^* | \langle \lambda j_f | \hat{M}_J | d \rangle |^2 \right. \\ & + j_3 j_3^* | \langle \lambda j_f | \hat{L}_J | d \rangle |^2 + 2\Re(j_0 j_3^* \langle \lambda j_f | \hat{M}_J | d \rangle \langle \lambda j_f | \hat{L}_J | d \rangle^*)] \\ & + \frac{1}{2} (\vec{j} \cdot \vec{j}^* - j_3 j_3^*) \sum_{\lambda j_f, J \geq 1} [ | \langle \lambda j_f | \hat{T}_J^{mag} | d \rangle |^2 + | \langle \lambda j_f | \hat{T}_J^{el} | d \rangle |^2 ] \\ & \left. + i(\vec{j} \times \vec{j}^*)_3 \sum_{\lambda j_f, J \geq 1} \Im(\langle \lambda j_f | \hat{T}_J^{mag} | d \rangle \langle \lambda j_f | \hat{T}_J^{el} | d \rangle^*) \right\}. \quad (4.5) \end{aligned}$$

Here  $G_W = G_F$  for the neutral channel reactions (4.1), (4.2), whereas  $G_W = G_F \cos \theta_C$  for the charged channel reactions (4.3), (4.4),  $G_F$  is the Fermi constant and  $\theta_C$  is the Cabibbo

angle. Further, the relative momentum of the nucleons in the final state is

$$\kappa_0 = \sqrt{2M_r(k - E'_l - \Delta) - \frac{1}{4}|\vec{q}|^2}, \quad (4.6)$$

where  $M_r$  is the reduced mass of the nucleons,  $\vec{k}(\vec{k}')$  is the momentum of the incoming (anti)neutrino (outgoing lepton),  $E'_l = \sqrt{m_l^2 + (\vec{k}')^2}$  is the energy of the final lepton. For the reactions (4.1) and (4.2),

$$\Delta = |\epsilon_d| = 2.2245 \text{ MeV}, \quad (4.7)$$

whereas for the reaction (4.3),

$$\Delta = M_p - M_n + |\epsilon_d| = 0.9312 \text{ MeV}, \quad (4.8)$$

and for the reaction (4.4),

$$\Delta = M_n - M_p + |\epsilon_d| = 3.5178 \text{ MeV}. \quad (4.9)$$

The 4-momentum transfer is

$$\vec{q} = \vec{k} - \vec{k}', \quad q_0 = k - E'_l. \quad (4.10)$$

For the neutral current reactions, Eqs. (4.1) and (4.2),

$$k'_{max} = kx - 4M_r + \left[ 8M_r(2M_r - \Delta + k(1 - x)) + k^2(x^2 - 1) \right]^{\frac{1}{2}}. \quad (4.11)$$

For the charged channel reactions, Eqs. (4.3) and (4.4), the upper limit of the final lepton momentum,  $k'_{max}$ , is provided by the solution of the equation

$$(\vec{k} - \vec{k}')^2 + 8M_r(E'_l + \Delta - k) = 0. \quad (4.12)$$

The lepton form factors entering Eq. (4.5) are given by the following equations

$$\frac{1}{2}(\vec{j} \cdot \vec{j}^* - j_3 j_3^*) = 2[1 - (\hat{k} \cdot \hat{q})(\vec{\beta} \cdot \hat{q})] \rightarrow \frac{4 \sin^2 \frac{\theta}{2}}{|\vec{q}|^2} [|\vec{q}|^2 + 2kk' \cos^2 \frac{\theta}{2}], \quad (4.13)$$

$$j_3 j_3^* = 2[1 - (\vec{\beta} \cdot \hat{k}) + 2(\hat{k} \cdot \hat{q})(\vec{\beta} \cdot \hat{q})] \rightarrow \frac{4q_0^2 \cos^2 \frac{\theta}{2}}{|\vec{q}|^2}, \quad (4.14)$$

$$j_0 j_0^* = 2[1 + (\vec{\beta} \cdot \hat{k})] \rightarrow 4 \cos^2 \frac{\theta}{2}, \quad (4.15)$$

$$j_0 j_3^* = 2\hat{q} \cdot (\hat{k} + \vec{\beta}) \rightarrow \frac{4q_0}{|\vec{q}|} \cos^2 \frac{\theta}{2}, \quad (4.16)$$

$$i(\vec{j} \times \vec{j}^*)_3 = 4s\hat{q} \cdot (\hat{k} - \vec{\beta}) \rightarrow \frac{8s}{|\vec{q}|} \sin \frac{\theta}{2} \left[ q^2 \cos^2 \frac{\theta}{2} + |\vec{q}|^2 \sin^2 \frac{\theta}{2} \right]^{\frac{1}{2}}. \quad (4.17)$$

The form factors, presented after the arrows, are valid in the zero mass limit of the outgoing lepton. The vector  $\vec{\beta}$  and the unit vectors of the type  $\hat{b}$  are defined as

$$\vec{\beta} = \frac{\vec{k}'}{E'_l}, \quad \hat{b} = \frac{\vec{b}}{|\vec{b}|}. \quad (4.18)$$

In addition, in Eq.(4.17),  $s = -1(+1)$  for the reactions (4.1) and (4.3) ((4.2) and (4.4)). The form factors (4.13)-(4.16) are the same for all four studied reactions.

Let us note that for the reaction (4.3), the function under integral in Eq.(4.5) should be multiplied by the Fermi function. For the solar neutrinos, a good approximation for this function is [75]

$$F(Z, E) = \frac{2\pi\nu}{1 - \exp(-2\pi\nu)}, \quad \nu = \alpha Z \frac{E'}{k'}. \quad (4.19)$$

The reduced matrix elements in Eq.(4.5) read

$$\langle \lambda j_f || \hat{O}_J || d \rangle = \frac{\sqrt{4\pi}}{\kappa_0} \sum_{l', l_d} \int_0^\infty r^2 dr \frac{u_{l', \lambda}^{j_f}(\kappa_0; r)}{r} \langle (l' s) j_f || \hat{O}_J || (l_d 1) 1 \rangle \frac{u_{l_d}}{r}, \quad (4.20)$$

where the nucleon-nucleon partial waves have asymptotics

$$u_{l_s, \lambda}^j \rightarrow U_{l_s, \lambda}^j \sin(\kappa_0 r - \frac{l\pi}{2} + \delta_\lambda^j), \quad (4.21)$$

and the phase shifts and mixing parameters correspond to the Blatt–Biedenharn [91] convention.

The multipoles are defined as

$$\hat{T}_{lm}^{mag}(q) = \frac{(-i)^l}{4\pi} \int d\Omega_{\hat{q}} \vec{Y}_{lm}^l(\hat{q}) \cdot \vec{j}(\vec{q}), \quad (4.22)$$

$$\hat{T}_{lm}^{el}(q) = \frac{(-i)^{l-1}}{4\pi} \int d\Omega_{\hat{q}} \vec{Y}_{lm}^{(1)}(\hat{q}) \cdot \vec{j}(\vec{q}), \quad (4.23)$$

$$\hat{L}_{lm}(q) = -\frac{(-i)^l}{4\pi} \int d\Omega_{\hat{q}} \vec{Y}_{lm}^{(-1)}(\hat{q}) \cdot \vec{j}(\vec{q}), \quad (4.24)$$

$$\hat{M}_{lm} = \frac{(-i)^l}{4\pi} \int d\Omega_{\hat{q}} Y_{lm}(\hat{q}) j_0(\vec{q}), \quad (4.25)$$

where

$$\vec{Y}_{lm}^{(1)}(\hat{q}) = \sqrt{\frac{l+1}{2l+1}} \vec{Y}_{lm}^{l-1}(\hat{q}) + \sqrt{\frac{l}{2l+1}} \vec{Y}_{lm}^{l+1}(\hat{q}), \quad (4.26)$$

$$\vec{Y}_{lm}^{(-1)}(\hat{q}) = \sqrt{\frac{l}{2l+1}} \vec{Y}_{lm}^{l-1}(\hat{q}) - \sqrt{\frac{l+1}{2l+1}} \vec{Y}_{lm}^{l+1}(\hat{q}). \quad (4.27)$$

$$(4.28)$$

The weak hadron neutral current, triggering the reactions (4.1) and (4.2), is given by the equation

$$j_{NC, \mu} = (1 - 2\sin^2\theta_W) j_\mu^3 - 2\sin^2\theta_W j_{S\mu} + j_{5\mu}^3, \quad (4.29)$$

where  $\theta_W$  is the Weinberg angle [1] ( $\sin^2\theta_W = 0.23149(15)$  [92]),  $j_\mu^3$  ( $j_{5\mu}^3$ ) is the third component of the weak vector (axial) current in the isospin space, and  $j_{S\mu}$  is the isoscalar vector current. In its turn, the weak hadron charged current is

$$j_{CC, \mu}^a = j_\mu^a + j_{5\mu}^a. \quad (4.30)$$

At low energies, the space component of the weak axial hadron current is the most important one.

Our hadron currents consist of the one- and two-nucleon parts. The one-nucleon currents are of the form,

$$\vec{j}^a = \frac{1}{2M} [F_1^V \vec{P}_1 + iG_M^V (\vec{\sigma} \times \vec{q})] \frac{\tau^a}{2}, \quad (4.31)$$

$$\vec{j}_5^a = g_A F_A \left\{ \vec{\sigma} - \frac{1}{8M^2} [\vec{P}_1^2 \vec{\sigma} - (\vec{\sigma} \cdot \vec{P}_1) \vec{P}_1 + (\vec{\sigma} \cdot \vec{q}) \vec{q} - i(\vec{P}_1 \times \vec{q})] \right\} \frac{\tau^a}{2}. \quad (4.32)$$

As to the two-nucleon part, we consider the WANECs only. In addition to the new potential exchange currents  $\vec{j}_{5,\rho}^a(pot)$ ,  $\vec{j}_{5,\omega}^a(pair)$ , and the non-potential exchange current  $\vec{j}_{5,a_1\rho}^a(a_1)$ , we include in our calculations the following exchange currents, derived in the chiral invariant models [40, 42, 62]:

1. The  $\pi$  potential term,

$$\begin{aligned} \Delta \vec{j}_{5,\pi}^a(pv) &= \left(\frac{g}{2M}\right)^2 \frac{g_A}{2M} F_A(q^2) [(\vec{q} + i\vec{\sigma}_1 \times \vec{P}_1) \tau_2^a + (\vec{P}_1 + i\vec{\sigma}_1 \times \vec{q}) i(\vec{\tau}_1 \times \vec{\tau}_2)^a] \\ &\quad \times \Delta_F^\pi(\vec{q}_2^2) F_{\pi NN}^2(\vec{q}_2^2) (\vec{\sigma}_2 \cdot \vec{q}_2) + (1 \leftrightarrow 2). \end{aligned} \quad (4.33)$$

2. The  $\rho$ - $\pi$  current,

$$\begin{aligned} \vec{j}_{5,\pi}^a(\rho\pi) &= -\left(\frac{g}{2M}\right)^2 \frac{1}{4Mg_A} \left[1 + \frac{m_\rho^2}{m_\rho^2 + \vec{q}_1^2}\right] [\vec{P}_1 + (1 + \kappa_\rho^V) i(\vec{\sigma}_1 \times \vec{q}_1)] \\ &\quad \times F_{\rho NN}(\vec{q}_1^2) \Delta_F^\pi(\vec{q}_2^2) F_{\pi NN}(\vec{q}_2^2) (\vec{\sigma}_2 \cdot \vec{q}_2) i(\vec{\tau}_1 \times \vec{\tau}_2)^a + (1 \leftrightarrow 2) \end{aligned} \quad (4.34)$$

3. The  $\Delta$  excitation current of the pion range,

$$\begin{aligned} \vec{j}_{5,\pi}^a(\Delta) &= \frac{g_A}{9(M_\Delta - M)} F_A(q^2) \left(\frac{f_{\pi N\Delta}}{m_\pi}\right)^2 [4\vec{q}_2 \tau_2^a + i(\vec{\sigma}_1 \times \vec{q}_2) i(\vec{\tau}_1 \times \vec{\tau}_2)^a] \\ &\quad \times \Delta_F^\pi(\vec{q}_2^2) F_{\pi NN}^2(\vec{q}_2^2) (\vec{\sigma}_2 \cdot \vec{q}_2) + (1 \leftrightarrow 2). \end{aligned} \quad (4.35)$$

4. The  $\Delta$  excitation current of the  $\rho$  meson range,

$$\begin{aligned} \vec{j}_{5,\rho}^a(\Delta) &= -\frac{G_1 g_\rho^2 f_\pi}{9(M_\Delta - M)} \frac{f_{\pi N\Delta}}{m_\pi} \frac{1 + \kappa_\rho^V}{2M^2} [4\vec{q}_2 \times (\vec{\sigma}_2 \times \vec{q}_2) \tau_2^a + i\vec{\sigma}_1 \times (\vec{q}_2 \times (\vec{\sigma}_2 \times \vec{q}_2)) i(\vec{\tau}_1 \times \vec{\tau}_2)^a] \\ &\quad \times \Delta_F^\rho(\vec{q}_2^2) F_{\rho NN}^2(\vec{q}_2^2) + (1 \leftrightarrow 2). \end{aligned} \quad (4.36)$$

The form factors  $F_1^V$ ,  $G_M^V$ , and  $F_A$ , are chosen in accord with Ref. [12]. The deuteron wave function and the wave functions of the  $^1S_0$  and  $^3P_J$  states of the final nucleons are obtained by solving the Schrödinger equation, making use of the following first and second generation realistic potentials:

(i) The potential OBEPQB [93], extended to include the  $a_1$  meson exchange [94]. The form factors, entering the BNN vertices, are of the monopole (dipole) shape for the exchanged meson  $B=\pi(\rho, \omega, a_1)$ .

(ii) The Nijmegen 93 (Nijm93) and Nijmegen I (NijmI) potentials [95]. In these potentials, the exponential strong BNN form factors enter.

In order to keep our calculations consistent, we make use of the same BNN form factors also in the currents. The value of the  $\pi N\Delta$  coupling,  $f_{\pi N\Delta}^2/4\pi m_\pi^2=0.7827 \text{ fm}^{-2}$ , is derived from the  $\Delta$  isobar width and it is compatible with the pion photo- and electroproduction on the nucleon, the value of the constant  $G_1$ ,  $G_1=2.525$ , follows from the pion photo- and electroproduction [96], and  $\kappa_\rho^V=6.6$  [93].

In table 1, we present the scattering lengths and the effective ranges, obtained from the NijmI, Nijm93, OBEPQG and AV18\*\* [97] potentials, and also the values of these quantities, applied in the EFT calculations [75]. For the generation of the final state nucleon–nucleon wave functions from the NijmI and Nijm 93 potentials, we adopted the program COCHASE [98]. This program solves the Schrödinger equation by employing the fourth–order Runge–Kutta method. This can provide the low–energy scattering parameters slightly different from those, obtained by the Nijmegen group, which makes use of the modified Numerov method [99]. Some refit was necessary, in order to get the required low–energy scattering parameters in the neutron–proton and neutron–neutron  $^1S_0$  states.

Table 1. Scattering lengths and effective ranges (in fm) for the nucleon–nucleon system in the  $^1S_0$  state, corresponding to the NijmI, Nijm93 [95], OBEPQG [94], AV18 [97] potentials and as used in the EFT calculations [75], and the experimental values.

	NijmI	Nijm93	OBEPQG	AV18	EFT	exp.
$a_{np}$	-23.72	-23.74	-23.74	-23.73	-23.7	$-23.740\pm 0.020^1$
$r_{np}$	2.65	2.68	2.73	2.70	2.70	$2.77 \pm 0.05^1$
$a_{pp}$	-7.80	-7.79	-	-7.82	-7.82	$-7.8063\pm 0.0026^2$
$r_{pp}$	2.74	2.71	-	2.79	2.79	$2.794\pm 0.014^2$
$a_{nn}$	-18.16	-18.11	-18.10	-18.49	-18.5	$-18.59\pm 0.40^3$
$r_{nn}$	2.80	2.78	2.77	2.84	2.80	$2.80\pm 0.11^4$

<sup>1</sup> Ref. [100]; <sup>2</sup> Ref. [101]; <sup>3</sup> Ref. [102]; <sup>4</sup> Ref. [103]

Below, we compare our numerical results for the cross sections with those obtained in the pionless EFT [75] and in the models, developed within the SNPA [12, 80, 81]. However, in order to make the comparison with the Ref. [75], one needs to know the constant  $L_{1,A}$ , entering the cross sections of the pionless EFT. In the next section, we extract it from the numerical values of the cross sections, obtained in various potential models.

## B. Extraction of the low energy constant $L_{1,A}$

In Ref. [75], the effective cross sections for the reactions (4.1)–(4.4) are presented in the form

$$\sigma_{EFT}(E_\nu) = a(E_\nu) + L_{1,A} b(E_\nu). \quad (4.37)$$

The amplitudes  $a(E_\nu)$  and  $b(E_\nu)$  are tabulated in [75] for each of the reactions (4.1)–(4.4), from the lowest possible (anti)neutrino energy up to 20 MeV. The constant  $L_{1,A}$  cannot be determined from reactions between elementary particles. In our analysis [104], we extracted  $L_{1,A}$  from our cross sections, calculated in the same approximation, as it was used in Ref. [75]: only the  $^1S_0$  wave was taken into account in the nucleon–nucleon final states and the nucleon

---

\*\* This potential is used in Ref. [80].

variables were treated non-relativistically. The knowledge of  $L_{1,A}$  allowed us to compare our cross sections with  $\sigma_{EFT}(E_\nu)$ . The results showed that the EFT cross sections were in better agreement with the cross sections of Ref. [80], even though Nakamura *et al.* took into account also the contribution from the  ${}^3P_J$  waves and treated the phase space relativistically. We defined the extracted value of the constant  $L_{1,A}$  as an average value,  $\bar{L}_{1,A}$ , according to the equation

$$\bar{L}_{1,A} = \frac{\sum_{i=1}^N L_{1,A}(i)}{N}, \quad L_{1,A}(i) = \frac{\sigma_{pot,i} - a_i}{b_i}, \quad (4.38)$$

where  $\sigma_{pot,i}$  is the cross section, calculated in the potential model and for the  $i$ -th (anti)neutrino energy. The application of the same equation in the present calculations yields the values of  $\bar{L}_{1,A}$ , presented in table 2. As it is seen from table 2, the variation of  $\bar{L}_{1,A}$  is about 10 % for the neutral current reactions, whereas it is up to 40 % for the charged current reactions.

Let us note that the values of the constant  $L_{1,A}$ , obtained from various analyses [105, 106], are charged with large errors. E.g., the analysis [106] of the data provided by the experiments with the reactor antineutrino beams yielded  $\bar{L}_{1,A} = 3.6 \pm 5.5 \text{ fm}^3$ .

Table 2. Values of the constant  $\bar{L}_{1,A}$  (in  $\text{fm}^3$ ), extracted from the cross sections of the reactions (4.1)-(4.4), which were calculated with the NijmI, Nijm93, and OBEPQG potentials, and from the cross sections NSGK taken from table I of Ref.[80].

reaction	NijmI	Nijm93	OBEPQG	NSGK
(4.1)	4.8	5.4	5.0	5.4
(4.2)	5.2	5.8	5.4	5.5
(4.3)	4.4	5.3	-	6.0
(4.4)	4.8	5.7	7.2	5.6

In the next section, employing the extracted values of the constant  $\bar{L}_{1,A}$ , we compare our cross sections with those of the pionless EFT [75], and also with the cross sections of Refs. [12, 80, 81].

### C. Comparison of the cross sections

For the comparison presented in table 3 and table 4, we employ the cross sections calculated with the nuclear wave functions generated from the NijmI potential. In comparing our results with those of Ref. [75] we make use of the values of the weak interaction constants  $G_F = 1.166 \times 10^{-5} \text{ GeV}^{-2}$  and  $g_A = -1.26$ , but we adopt the value  $g_A = -1.254$  when comparing with Refs. [80, 81]. In the calculations of the cross sections for the charged channel reactions (4.3) and (4.4), the value of the Cabibbo angle is taken  $\cos\theta_C = 0.975$ .

Table 3. Cross sections and the differences in % between the cross sections for the reactions (4.1) and (4.2). The first 7 columns is related to the reaction (4.1). In the first column,  $E_\nu$  [MeV] is the neutrino energy, in the second column,  $\sigma_{NijmI}$  (in  $10^{-42} \times \text{cm}^2$ ) is the cross section, calculated with the NijmI nuclear wave functions. Column 3 reports the difference between  $\sigma_{NijmI}$  (NijmI) and the EFT cross section (4.37)  $\sigma_{EFT}$ , calculated with the corresponding constant  $\bar{L}_{1,A}$  of table 2. The difference between  $\sigma_{NSGK}$ , taken from table I of Ref. [80], and  $\sigma_{EFT}$ , is reported in column 4. Further,  $\Delta_{1(2)}$  is the difference between the cross sections  $\sigma_{NijmI}$  ( $\sigma_{Nijm93}$ ) and  $\sigma_{NSGK}$ ;  $\Delta_3$  is the difference between the cross sections

$\sigma_{NijmI}$  and  $\sigma_{YHH}$ , where the cross section  $\sigma_{YHH}$  is taken from table I of Ref. [81]. The second part of the table is an analogue for the reaction (4.2).

$\nu_x + d \longrightarrow \nu_x' + n p$							$\bar{\nu}_x + d \longrightarrow \bar{\nu}_x' + n p$						
$E_\nu$	$\sigma_{NijmI}$	NijmI	NSGK	$\Delta_1$	$\Delta_2$	$\Delta_3$	$E_{\bar{\nu}}$	$\sigma_{NijmI}$	NijmI	NSGK	$\Delta_1$	$\Delta_2$	$\Delta_3$
3	0.00335	1.0	0.4	-1.1	-0.5	-	3	0.00332	0.3	0.1	-1.1	-0.5	-
4	0.0306	1.0	0.2	-0.8	-0.2	12.0	4	0.0302	0.7	0.2	-0.8	-0.1	9.3
5	0.0948	1.0	0.2	-0.9	-0.2	5.0	5	0.0929	0.7	0.1	-0.8	-0.1	0.9
6	0.201	0.8	0.1	-1.0	-0.3	10.2	6	0.196	0.8	0.3	-0.8	-0.1	5.8
7	0.353	0.8	0.1	-1.1	-0.3	8.2	7	0.342	0.5	0.1	-0.9	-0.2	2.0
8	0.552	0.7	0.2	-1.2	-0.4	10.1	8	0.532	1.1	0.8	-1.0	-0.2	3.2
9	0.799	0.8	0.4	-1.3	-0.5	9.0	9	0.766	0.6	0.2	-1.1	-0.3	1.0
10	1.095	0.2	-0.1	-1.4	-0.6	7.8	10	1.045	0.4	0.2	-1.2	-0.4	-1.5
11	1.441	0.6	0.5	-1.6	-0.8	9.6	11	1.368	-0.1	-0.2	-1.3	-0.5	-0.4
12	1.836	-0.2	-0.3	-1.8	-0.9	8.8	12	1.734	-0.3	-0.4	-1.4	-0.5	-2.5
13	2.282	-0.1	0.0	-1.9	-1.1	10.2	13	2.144	-0.3	-0.2	-1.5	-0.6	-1.7
14	2.779	-0.3	0.0	-2.1	-1.2	9.9	14	2.597	-0.4	-0.2	-1.6	-0.7	-3.4
15	3.326	-0.6	-0.1	-2.3	-1.4	10.8	15	3.092	-0.5	-0.2	-1.8	-0.9	-3.5
16	3.923	-0.9	-0.3	-2.5	-1.6	10.5	16	3.628	-0.6	-0.1	-1.9	-1.0	-4.9
17	4.571	-1.2	-0.4	-2.7	-1.8	11.2	17	4.206	-0.8	-0.2	-2.1	-1.1	-5.2
18	5.269	-1.4	-0.3	-3.0	-2.0	11.1	18	4.824	-1.0	-0.3	-2.3	-1.3	-6.6
19	6.017	-1.7	-0.4	-3.2	-2.2	10.6	19	5.481	-1.3	-0.3	-2.5	-1.5	-6.9
20	6.814	-2.1	-0.6	-3.5	-2.5	11.7	20	6.177	-1.4	-0.2	-2.7	-1.6	-8.1

Comparing this table with table 3 and table 4 of Ref. [104] we conclude that the effect of the  ${}^3P_J$  waves leads our cross sections in better agreement with the EFT cross sections, but the effect is weaker in comparison with the one obtained in Ref. [80]. On the other hand, the disagreement with the cross sections of Ref. [81] is even more pronounced at higher energies. Table 3 also shows that our cross sections are in better agreement with the other cross sections in the case of the reaction (4.2), than in the case of the reaction (4.1). One can also conclude from the differences, given in the columns NijmI, NSGK,  $\Delta_1$ , and  $\Delta_2$  that the cross sections for the reactions (4.1) and (4.2) are described by both the potential models and the pionless EFT with an accuracy better than 3%.

In table 4, we present the comparison of the cross sections for the reactions in the charged channel.

Table 4. Cross sections and the differences in % between cross sections for the reactions (4.3) and (4.4). For notations, see table 3.

$\nu_e + d \longrightarrow e^- + pp$							$\bar{\nu}_e + d \longrightarrow e^+ + nn$						
$E_\nu$	$\sigma_{NijmI}$	NijmI	NSGK	$\Delta_1$	$\Delta_2$	$\Delta_3$	$E_{\bar{\nu}}$	$\sigma_{NijmI}$	NijmI	NSGK	$\Delta_1$	$\Delta_2$	$\Delta_3$
2	0.00338	-5.8	-0.6	-7.6	-6.7	-	-	-	-	-	-	-	-
3	0.0455	-0.8	-0.3	-3.0	-2.0	-	-	-	-	-	-	-	-
4	0.153	0.1	-0.6	-1.9	-0.9	1.9	-	-	-	-	-	-	-
5	0.340	1.1	0.1	-1.6	-0.6	2.9	5	0.0274	-1.7	-0.9	-2.5	-1.6	9.0
6	0.613	1.5	0.4	-1.5	-0.5	3.1	6	0.116	-0.3	-0.1	-2.1	-1.1	8.1
7	0.979	1.6	0.4	-1.5	-0.5	3.1	7	0.277	-0.1	-0.2	-1.8	-0.7	7.4
8	1.440	-0.4	-2.4	-1.6	-0.6	3.3	8	0.514	0.2	-0.1	-1.6	-0.5	7.1
9	2.000	-0.6	-2.3	-1.7	-0.6	3.1	9	0.830	0.1	-0.2	-1.6	-0.5	7.0
10	2.662	-0.2	-1.7	-1.9	-0.7	3.3	10	1.226	0.7	0.3	-1.6	-0.4	6.9
11	3.426	3.4	3.3	-2.0	-0.9	3.1	11	1.701	0.6	0.2	-1.6	-0.5	6.2
12	4.294	1.0	0.3	-2.2	-1.1	2.9	12	2.255	0.5	0.1	-1.6	-0.5	6.4
13	5.268	0.8	0.2	-2.4	-1.3	2.9	13	2.887	0.3	0.0	-1.7	-0.6	5.9
14	6.348	0.5	0.2	-2.7	-1.5	2.7	14	3.596	0.4	0.2	-1.8	-0.6	5.6
15	7.535	0.3	0.2	-2.9	-1.7	2.4	15	4.380	0.1	0.0	-2.0	-0.7	5.5
16	8.829	-0.1	-0.1	-3.1	-2.0	2.2	16	5.237	0.1	0.1	-2.1	-0.9	5.3
17	10.23	-0.5	-0.1	-3.5	-2.3	1.9	17	6.167	0.0	0.2	-2.3	-1.0	4.4
18	11.74	-0.8	-0.1	-3.8	-2.6	1.1	18	7.168	0.1	0.4	-2.4	-1.1	4.2
19	13.36	-1.0	-0.0	-4.1	-2.9	1.0	19	8.237	-0.2	0.2	-2.6	-1.3	3.9
20	15.09	-1.5	-0.3	-4.4	-3.2	1.0	20	9.373	-0.3	0.3	-2.8	-1.5	3.7

It can be seen from the left-hand part of table 4 that our cross sections and the cross section [80] are smooth functions of the neutrino energy, whereas the EFT cross section exhibits abrupt changes in the region  $7 < E_\nu < 12$  MeV. In our opinion, the reason can be in an incorrect treatment of the Coulomb interaction between protons in the EFT calculations. It follows from the right-hand part of table 4 that our cross sections and also the cross sections by Nakamura *et al.* [80] are in very good agreement with the EFT cross sections, in spite of the fact that the difference up to 3 % between these calculations persists. Large difference between our calculations and those by Ying *et al.* at the threshold energies can be understood by a poor description of the neutron–neutron low energy scattering parameters by the Paris potential model.

Next we compare our cross sections with those of Ref. [12]. For this purpose, we use  $G_F = 1.1803 \times 10^{-5}$  GeV<sup>-2</sup> and  $g_A = -1.267$ . The results, displayed in table 5 are for the reaction (4.1) and the OBEPQG potential. The parameters of this potential, required in the calculations of the exchange current effects, are  $g_{\pi NN}^2/4\pi=14.4$ ,  $g_{\rho NN}^2/4\pi=3.6$ ,  $g_{\omega NN}^2/4\pi=98$ ,  $\Lambda_\pi=8.62$  fm<sup>-1</sup>,  $\Lambda_\rho=\Lambda_\omega=9.38$  fm<sup>-1</sup>, and  $\Lambda_{a_1}=10.14$  fm<sup>-1</sup>. The shape of the table enables one to compare our calculations directly with those, presented in table 1 and table 3 of Ref. [12]. It follows from table 5 that the most important contributions to the cross section are from the  $\Delta$  excitation currents and from other currents of the pion range. It is also seen that the contributions from the  $\pi$  potential- and the  $\rho$ - $\pi$  terms compensate each other to a large extent [62]. One can also see that the currents interfere between themselves destructively. Besides, the contributions from the heavy meson exchange currents, such as the  $\rho$  potential term, the  $\omega$  pair- and  $a_1$ - $\rho$  currents, are at the threshold energies numerically insignificant. In the last row, we present the cross sections due to the transition  ${}^3S_1 - {}^3D_1 \rightarrow {}^1S_0$  only.

The comparison of the last two rows shows that the effect of the  ${}^3P_J$  interaction in the final state is  $\approx 0.2/0.6/1.2\%$  at  $E_\nu = 10/15/20$  MeV.

Table 5. Cumulative contributions to the cross section  $\sigma_{\nu d}$  ( $\times 10^{-42}$  cm $^2$ ) from the weak axial exchange currents for various neutrino energies are displayed. The cross section, calculated in the impulse approximation (including the relativistic corrections of the order  $\mathcal{O}(1/M^2)$ ) is presented in the row labelled as IA ( $\delta$ IA). Other contributions correspond to the exchange currents as follows:  $\Delta(\pi) \rightarrow \vec{j}_{5,\pi}^3(\Delta)$ ;  $\Delta(\rho) \rightarrow \vec{j}_{5,\rho}^3(\Delta)$ ;  $p(\pi) \rightarrow \Delta \vec{j}_{5,\pi}^a(pv)$ ;  $p(\rho) \rightarrow \vec{j}_{5,\rho}^3(pot)$ ;  $p(\omega) \rightarrow \vec{j}_{5,\omega}^3(pair)$ ;  $\rho-\pi \rightarrow \vec{j}_{5,\pi}^3(\rho\pi)$ ;  $a_1-\rho \rightarrow \vec{j}_{5,a_1\rho}^3(a_1)$ . The cross section in the n-th row is given by the contribution of all previous currents, the n-th current including. The number in the bracket is the ratio of the n-th cross section to the cross section in the row above. The first three exchange current contributions are from the long-range exchange currents. The cross sections in the last row are obtained with the neutron-proton wave function calculated only for the transition  ${}^3S_1 - {}^3D_1 \rightarrow {}^1S_0$ .

$E_\nu$ [MeV]	5	10	15	20
IA	0.0948 (-)	1.088(-)	3.296 (-)	6.740 (-)
+ $\delta$ IA	0.0944 (0.997)	1.084 (0.996)	3.281 (0.995)	6.709 (0.995)
+ $\Delta(\pi)$	0.0996 (1.055)	1.151 (1.062)	3.499 (1.067)	7.175 (1.070)
+p( $\pi$ )	0.0989 (0.992)	1.141 (0.991)	3.466 (0.991)	7.010 (0.990)
+ $\rho-\pi$	0.0997 (1.008)	1.152 (1.010)	3.502 (1.010)	7.181 (1.011)
+ $\Delta(\rho)$	0.0983 (0.986)	1.134 (0.984)	3.444 (0.983)	7.056 (0.983)
+p( $\rho$ )	0.0986 (1.003)	1.137 (1.003)	3.455 (1.003)	7.079 (1.003)
+p( $\omega$ )	0.0986 (1.000)	1.138 (1.001)	3.456 (1.001)	7.083 (1.001)
+ $a_1-\rho$	0.0985 (0.999)	1.136 (0.999)	3.452 (0.999)	7.074 (0.999)
$\sigma({}^1S_0)$	0.0984	1.134	3.432	6.993

However, the currents, adopted in Ref. [12] differ from our currents in several aspects:

1. The  $\pi$  pair term is constructed from the pseudoscalar  $\pi NN$  coupling. This makes the model incompatible with the chiral invariance.
2. The  $\rho-\pi$  current, used in [12], is connected to our current (4.34) by the change

$$1 + \frac{m_\rho^2}{m_\rho^2 + \vec{q}_1^2} \rightarrow \frac{2m_\rho^2}{m_\rho^2 + \vec{q}_1^2}. \quad (4.39)$$

3. The  $\Delta$  excitation currents (4.35) and (4.36) are in [12] supplied with the couplings of the constituent quark model, additionally multiplied by a factor 0.8. This factor was found to be needed to obtain the experimental value of the Gamow-Teller matrix element for the triton  $\beta$  decay [44]. However, this way of fixing the MECs is a model dependent procedure depending on the specific choice of the nuclear model which is the AV18 potential in this case. Let us note that the exchange current model [12, 44] underestimates [107] the precise data on the ordinary muon capture in  ${}^3\text{He}$ ,  $\mu^- + {}^3\text{He} \rightarrow \nu_\mu + {}^3\text{H}$ . Besides, the resulting  $\pi N\Delta$  coupling is in a sharp contradiction with its value obtained from the  $\Delta$  width and also from the pion photo- and electroproduction on the nucleon. On the other hand, the damping factor  $M/M_\Delta \approx 0.8$  arises in the vector and axial  $\Delta$  excitation currents, if they are constructed from the

'gauge symmetric' Lagrangians [108, 109]. It means that in order to be consistent, one should repeat the analysis of the reaction  $n + p \rightarrow d + \gamma$  [80] with the damped vector  $\Delta$  excitation currents and make use of them also in [12]. Let us note that other possibility to reconcile the Gamow–Teller matrix element of the triton  $\beta$  decay with the data is to vary the cutoff parameters  $\Lambda_\pi$  and  $\Lambda_\rho$  [110], keeping the couplings of the  $\Delta$  excitation currents fixed.

4. The structure of our  $\rho$  potential term is different from the  $\rho$  pair term [12], and the  $\omega$  pair term and the  $a_1$ - $\rho$  current are in [12] absent.
5. The BNN vertices are of the monopole shape.
6. As it has been discussed in [62], it is not clear which nuclear continuity equation the currents [12, 44] satisfy.

In table 6, we present the results of calculations obtained with our currents modified according to points 2, 3 and 5 above and with the values of the parameters [12]  $g_{\pi NN}^2/4\pi=14.81$ ,  $g_{\rho NN}^2/4\pi=2.0$ ,  $f_{\pi N\Delta}^2/4\pi m_\pi^2=0.4701 \text{ fm}^{-2}$ ,  $\Lambda_\pi=4.8 \text{ fm}^{-1}$ ,  $\Lambda_\rho=6.8 \text{ fm}^{-1}$ .

In comparing our table 6 with table 3/Model I of Ref. [12], we mention our stronger  $\pi$  potential term and weaker  $\rho$  potential- and  $\rho$ - $\pi$  terms. Moreover, the  $\pi$ - and  $\rho$  potential terms are of the opposite sign in comparison with the  $\pi$ - and  $\rho$  pair terms of Ref.[12].

The comparison of our  $\rho$ - $\pi$  row of table 6 with the rows labelled as NPC Bonn and NPC AV18 shows that our results are by 1% to 2% smaller, while the same comparison in table 5 exhibits an opposite effect.

Table 6. Cumulative contributions to the cross section  $\sigma_{\nu d} (\times 10^{-42} \text{ cm}^2)$  from the modified weak axial exchange currents for various neutrino energies. For the notations, see table 5. The modification of the currents and the choice of the parameters are described in the text. The values of the cross sections in the rows labelled as NPC Bonn and NPC AV18 are displayed for comparison [111]. These cross sections correspond to the calculations [12], restricted to the transition  ${}^3S_1$ - ${}^3D_1 \rightarrow {}^1S_0$ , and for the CD-Bonn [100], and the AV18 [97] potentials, respectively.

$E_\nu$ [MeV]	5	10	15	20
IA	0.0948 (-)	1.088(-)	3.296 (-)	6.741 (-)
+ $\delta$ IA	0.0944 (0.997)	1.084 (0.996)	3.281 (0.995)	6.709 (0.995)
+ $\Delta(\pi)$	0.0962 (1.019)	1.107 (1.021)	3.356 (1.023)	6.869 (1.024)
+p( $\pi$ )	0.0956 (0.994)	1.099 (0.993)	3.331 (0.992)	6.814 (0.992)
+ $\rho$ - $\pi$	0.0957 (1.001)	1.100 (1.001)	3.334 (1.001)	6.821 (1.001)
+ $\Delta(\rho)$	0.0955 (0.997)	1.097 (0.997)	3.323 (0.997)	6.798 (0.997)
+p( $\rho$ )	0.0956 (1.001)	1.099 (1.002)	3.329 (1.002)	6.810 (1.002)
+p( $\omega$ )	0.0957 (1.001)	1.099 (1.000)	3.332 (1.001)	6.816 (1.001)
+ $a_1$ - $\rho$	0.0956 (0.999)	1.099 (1.000)	3.330 (1.000)	6.813 (1.000)
$\sigma({}^1S_0)$	0.0956	1.097	3.311	6.732
NPC Bonn	0.09552	1.099	3.323	6.765
NPC AV18	0.09565	1.101	3.332	6.787

Comparing table 6 with table 5 one concludes that in this model, the exchange effect is much weaker. Now also the  $\rho$ - $\pi$  current is numerically insignificant.

Besides the calculations presented in table 5 and table 6, that are obtained for the reaction (4.1) with the OBEPQG wave functions, we calculated also the cumulative cross sections for all the reactions (4.1)-(4.4) using the wave functions generated from the NijmI potential [95]. The results are presented in tables 7, 8, 9 and 10. In this case, we chose the couplings  $G_F$ ,  $g_A$  and  $\cos\theta_C$  according to Refs. [112],[113],

$$G_F = 1.16637(1) \times 10^{-5} GeV^{-2}, \quad g_A = -1.2720(8), \quad \cos\theta_C = 0.9730 \pm 0.0004 \pm 0.0012 \pm 0.0002. \quad (4.40)$$

Here the Fermi constant  $G_F$  is fixed by the muon decay. Making use of this value of  $G_F$ , the constants  $g_A$  and  $\cos\theta_C$  are extracted from the neutron beta decay.

Table 7. Cumulative contributions to the cross section  $\sigma_{\nu d}$  ( $\times 10^{-42}$  cm<sup>2</sup>) for the reaction (4.1), calculated with the nuclear wave functions and couplings and cutoffs, entering the axial exchange current operators, that correspond to the NijmI potential, for various neutrino energies. For the notations, see table 3.

$E_\nu$ [MeV]	5	10	15	20
IA	0.0927 (-)	1.065(-)	3.227 (-)	6.599 (-)
+ $\delta$ IA	0.0923 (0.996)	1.061 (0.996)	3.212 (0.995)	6.567 (0.995)
+ $\Delta(\pi)$	0.0977 (1.057)	1.130 (1.065)	3.436 (1.070)	7.047 (1.073)
+p( $\pi$ )	0.0969 (0.992)	1.119 (0.991)	3.401 (0.990)	6.972 (0.989)
+ $\rho$ - $\pi$	0.0977 (1.009)	1.131 (1.010)	3.439 (1.011)	7.051 (1.011)
+ $\Delta(\rho)$	0.0962 (0.984)	1.111 (0.982)	3.374 (0.981)	6.912 (0.980)
+p( $\rho$ )	0.0965 (1.003)	1.114 (1.003)	3.384 (1.003)	6.934 (1.003)
+p( $\omega$ )	0.0966 (1.002)	1.116 (1.002)	3.392 (1.002)	6.951 (1.002)
$\sigma(^1S_0)$	0.0966	1.114 (99.8)	3.372 (99.4)	6.868 (98.8)

Table 8. Cumulative contributions to the cross section  $\sigma_{\bar{\nu} d}$  ( $\times 10^{-42}$  cm<sup>2</sup>) for the reaction (4.2), calculated with the nuclear wave functions and couplings and cutoffs, entering the axial exchange current operators, that correspond to the NijmI potential, for various antineutrino energies. For the notations, see table 3.

$E_{\bar{\nu}}$ [MeV]	5	10	15	20
IA	0.0908 (-)	1.016(-)	2.996 (-)	5.972 (-)
+ $\delta$ IA	0.0905 (0.996)	1.011 (0.996)	2.982 (0.995)	5.942 (0.995)
+ $\Delta(\pi)$	0.0957 (1.058)	1.079 (1.067)	3.198 (1.072)	6.398 (1.077)
+p( $\pi$ )	0.0949 (0.992)	1.069 (0.990)	3.165 (0.990)	6.327 (0.989)
+ $\rho$ - $\pi$	0.0958 (1.009)	1.080 (1.011)	3.201 (1.011)	6.402 (1.012)
+ $\Delta(\rho)$	0.0943 (0.984)	1.060 (0.982)	3.138 (0.980)	6.270 (0.979)
+p( $\rho$ )	0.0945 (1.003)	1.064 (1.003)	3.148 (1.003)	6.291 (1.003)
+p( $\omega$ )	0.0947 (1.002)	1.066 (1.002)	3.156 (1.002)	6.307 (1.003)
$\sigma(^1S_0)$	0.0947	1.064 (99.8)	3.136 (99.4)	6.225 (98.7)

Table 9. Cumulative contributions to the cross section  $\sigma_{\nu d}$  ( $\times 10^{-42}$  cm<sup>2</sup>) for the reaction (4.3), calculated with the nuclear wave functions and couplings and cutoffs, entering the axial exchange current operators, that correspond to the NijmI potential, for various neutrino energies. For the notations, see table 3.

$E_{\bar{\nu}}$ [MeV]	5	10	15	20
IA	0.3320 (-)	2.587(-)	7.300 (-)	14.59 (-)
+ $\delta$ IA	0.3309 (0.997)	2.577 (0.996)	7.269 (0.996)	14.52 (0.995)
+ $\Delta(\pi)$	0.3481 (1.052)	2.729 (1.059)	7.730 (1.063)	15.49 (1.066)
+p( $\pi$ )	0.3458 (0.993)	2.708 (0.992)	7.666 (0.992)	15.35 (0.991)
+ $\rho$ - $\pi$	0.3491 (1.010)	2.737 (1.011)	7.752 (1.011)	15.53 (1.012)
+ $\Delta(\rho)$	0.3438 (0.985)	2.690 (0.983)	7.611 (0.982)	15.23 (0.981)
+p( $\rho$ )	0.3447 (1.003)	2.698 (1.003)	7.635 (1.003)	15.28 (1.003)
+p( $\omega$ )	0.3452 (1.001)	2.703 (1.002)	7.649 (1.002)	15.31 (1.002)
$\sigma(^1S_0)$	0.3451	2.696 (99.7)	7.597 (99.3)	15.12 (99.8)

Table 10. Cumulative contributions to the cross section  $\sigma_{\nu d}$  ( $\times 10^{-42}$  cm<sup>2</sup>) for the reaction (4.4), calculated with the nuclear wave functions and couplings and cutoffs, entering the axial exchange current operators, that correspond to the NijmI potential, for various antineutrino energies. For the notations, see table 3.

$E_{\bar{\nu}}$ [MeV]	5	10	15	20
IA	0.0268 (-)	1.190(-)	4.233 (-)	9.031 (-)
+ $\delta$ IA	0.0267 (0.997)	1.185 (0.996)	4.213 (0.995)	8.985 (0.995)
+ $\Delta(\pi)$	0.0281 (1.051)	1.259 (1.062)	4.505 (1.069)	9.653 (1.074)
+p( $\pi$ )	0.0279 (0.993)	1.249 (0.992)	4.464 (0.991)	9.559 (0.990)
+ $\rho$ - $\pi$	0.0281 (1.009)	1.263 (1.011)	4.518 (1.012)	9.680 (1.013)
+ $\Delta(\rho)$	0.0277 (0.985)	1.240 (0.982)	4.428 (0.980)	9.475 (0.979)
+p( $\rho$ )	0.0278 (1.002)	1.244 (1.003)	4.443 (1.003)	9.509 (1.004)
+p( $\omega$ )	0.0278 (1.000)	1.246 (1.002)	4.452 (1.002)	9.529 (1.002)
$\sigma(^1S_0)$	0.0278	1.244 (99.8)	4.426 (99.4)	9.407 (98.7)

It is seen from table 7–table 10 that again, the effects of the  $\pi$  potential- and  $\rho$ - $\pi$  terms compensate each other considerably. But in this potential model, the  $\rho$  potential- and  $\omega$  pair terms interfere additively and the sum of them contribute sensibly. The numbers in the brackets show the part (in %) of the  $^1S_0$  cross section from the total cross section.

In table 11, we compare the  $^1S_0$  phase shifts (in degrees) for the neutron–proton scattering obtained from different potentials, used in the calculations of the cross sections, presented above.

Table 11. Comparison of the  $^1S_0$  phase shift (in degrees) for the neutron–proton scattering described by the potentials CD-Bonn [100], OBEPQG [94], NijmI and Nijm93 [95].

$E_{lab}$ [MeV]	1	5	10	25	50
CD-Bonn	62.09	63.67	60.01	50.93	40.45
OBEPQG	62.02	63.56	59.91	50.82	40.13
NijmI	62.12	63.74	60.10	51.04	40.56
Nij93	62.05	63.61	59.94	50.85	40.38

The phase shifts labelled as CD-Bonn were delivered by R. Machleidt [114]. As it is seen, the resulting phase shifts are very close among themselves up to energies of 50 MeV. It means

that all four potentials are in the  $^1S_0$  channel about the same for the internucleon distances larger than 0.6 fm.

In Fig. 3, we consider for the reaction (4.1) and for the strongest multipole  $\hat{T}_1^{el}$  the ratios of the radial density for various exchange currents to the density of the  $\Delta$  excitation current of the pion range. As it is seen from Eq. (4.5), the densities depend on the cosine of the scattering angle,  $x = \cos \theta$ , and on the energy  $\nu'$  of the outgoing neutrino. In its turn,  $\nu'_{max}$  is given by the incident neutrino energy  $\nu$  and  $x$ . As it is seen from the figure, the ratios of the densities decrease substantially with increasing values of  $r$  for the short-range WANECs.

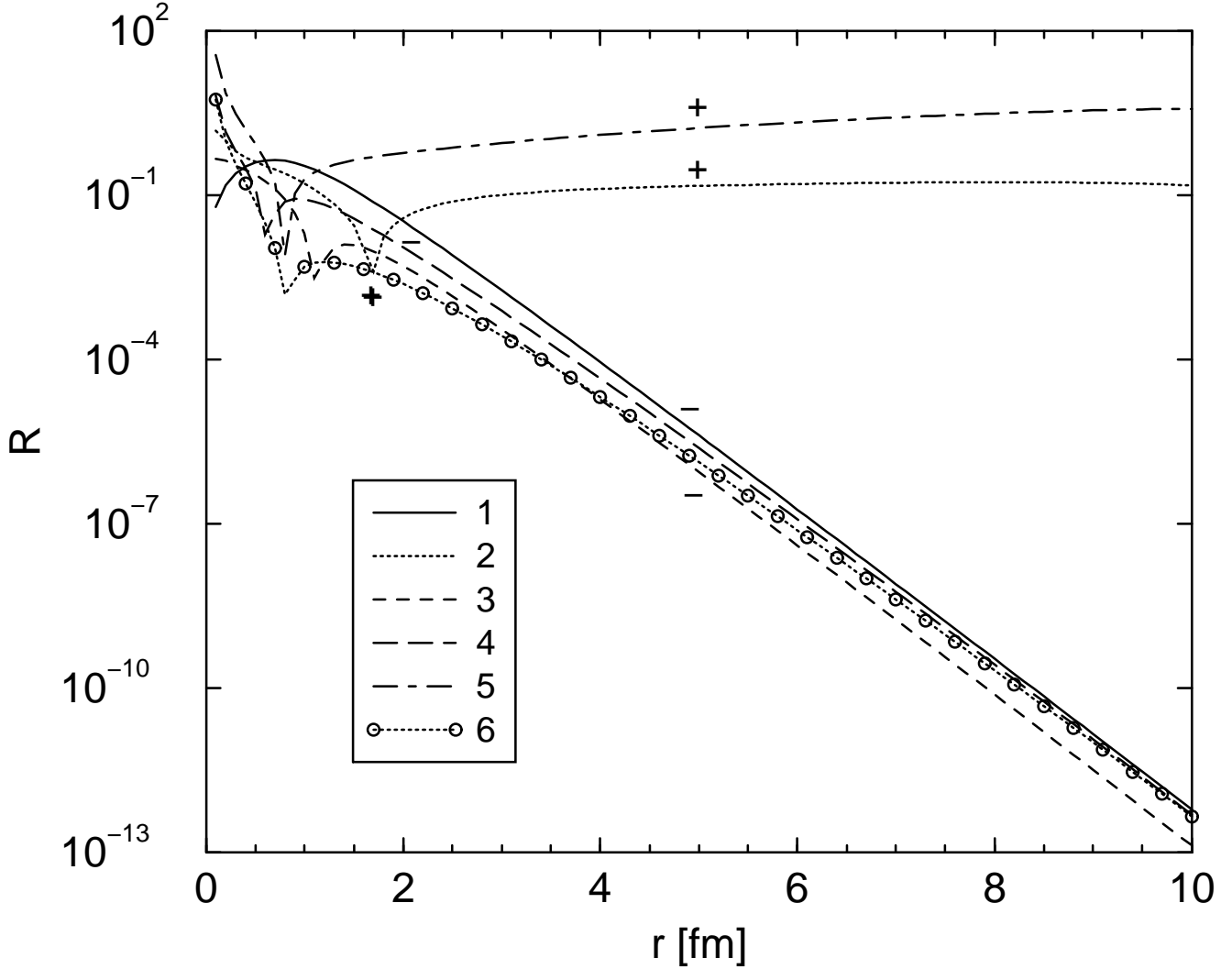


FIG. 3: The ratios of the radial density of various WANECs to the density of the  $\Delta$  excitation current of the pion range,  $\Delta(\pi)$ , are presented for the reaction (4.1), and for the  $\hat{T}_1^{el}$  multipole. The selected kinematics is  $\nu = 5$  MeV,  $\theta = 45^\circ$ ,  $\nu' = \nu'_{max}/2$ . With this choice, the momentum transfer is  $|\vec{q}| = 4.12$  MeV. The curves correspond to the following WANECs: 1-  $\Delta(\rho)$ , 2-  $p(\pi)$ , 3-  $p(\rho)$ , 4-  $p(\omega)$ , 5-  $\rho - \pi$ , 6-  $a_1 - \rho$ . The sign + (-) at a branch of a curve means that the ratio of the densities is positive (negative). The signs of the branches before and/or after the kinks are opposite.

## V. DISCUSSION OF OBTAINED RESULTS

In this paper, we construct the weak axial nuclear heavy meson exchange currents of the  $\rho^-$ ,  $\omega^-$  and  $a_1$  meson range in the TAA. These currents are suitable for calculations employing the nuclear wave functions obtained by solving the Schrödinger equation with the OBEPs. Including the  $\pi$  exchange current, our model currents provide the realistic space component of the axial exchange currents. Adopting for the exchange currents the needed input (couplings, cutoffs) from the OBEPs, we can make a reliable estimate of the effect due to these exchanges. Since our Lagrangians belong generically to the non-linear realization of the chiral group, the  $\sigma$  meson is explicitly lacking. On the other hand, the OBEPs contain the  $\sigma$  meson exchange, needed to explain the medium range attraction. Then it follows that the exchange effect, arising from this meson, cannot be calculated consistently in our approach. However, the structure of the space component of the WANECs of the  $\sigma$  range does not allow it to play any significant role at low energies. This is discussed in more detail in appendix B.

In accord with Ref. [58], we define the nuclear exchange currents in Eq. (3.1) as the difference of the relativistic Feynman amplitudes of Sect. II and of the first Born iteration of the nuclear equation of motion (3.2). The currents, derived in this manner, are given by a finite set of terms and they satisfy the nuclear PCAC equation (3.7). Let us note that our approach follows methods standardly used in the few-body nuclear physics at low and intermediate energies: the transition operator that is constructed for free nucleons is sandwiched between the nuclear wave functions obtained by solving the Schrödinger equation with realistic potentials. As is well known from the textbooks, if the transition operator is the sum of the one- and two-nucleon vector currents, it should satisfy the nuclear form of the CVC hypothesis (1.2). Then accepting chiral symmetry as one of the corner-stones on which the nuclear physics calculations rely, one should construct the axial currents satisfying the nuclear PCAC constraint, as it is done in this paper. If the particles cannot be considered as free (nuclear matter) or non-relativistic then one should use other methods to describe the nuclear states, and to construct the currents in conjunction with the relevant equation of motion for nuclear states, as it was done, e.g., in Ref. [50] for the axial currents and the Bethe-Salpeter equation, or in Refs. [115, 116] for the electromagnetic currents and the Blankenbecler-Sugar-Logunov-Tavkhelidze quasipotential equation.

After performing the standard non-relativistic reduction, we obtain the currents in the leading order in  $1/M$ . The non-zero difference arises due to the difference between the positive frequency part of the nucleon Born terms and of the first Born iteration, which gives rise to the vertex, external and retardation terms. The sum of the vertex terms and of the negative frequency Born terms (pair terms) results in the nuclear potential currents. The vertex currents contribute essentially in the case of the  $\pi^-$  and  $\rho$  meson exchanges. Note that the space parts of our  $\pi^-$  and  $\rho$  potential currents (3.27) differ from the space parts of the  $\pi^-$  and  $\rho$  pair terms, used in Refs. [12, 44, 45].

Besides the contribution from the nucleon Born terms, the potential contact and non-potential currents appear after the non-relativistic reduction. These currents have never been constructed before. An infinite set of such terms was supposed to exist in Ref. [45], where it was argued that these terms should be numerically insignificant because of the short-range suppression present in nuclear wave functions. We have shown here that the method based on the chiral invariance provides a finite set of terms, of which contributions can be estimated quantitatively.

The application of our currents to the reaction of weak deuteron disintegration by (anti)neutrinos at low energies shows that our currents differ from the set that has recently been used in Ref. [12], in that (i) The  $\pi$ - and  $\rho$  potential terms contribute with the opposite sign, in comparison with the  $\pi$ - and  $\rho$  pair terms [12], respectively. (ii) The effect of the  $\pi$  potential term cancels strongly the effect, arising from the  $\rho$ - $\pi$  current. Besides we have shown that at the threshold energies, the contributions to the cross sections from the heavy meson exchanges interfere destructively in conjunction with the OBEPQG potential, and the heavy meson effect is strongly suppressed in comparison with the effect arising from the currents of the pion range, as supposed in [45]. However, in conjunction with the potential NijmI, the  $\rho$  potential- and  $\omega$  pair terms interfere additively, and this sum is non-negligible. This result is important in particular in the case, if the  $\Delta$  isobar currents are adopted with the suppressed strength [12]. Such analysis can be performed for other potentials and/or energies, too, thus having bookkeeping of the exchange current effects under control. But at higher energies, other parts of our currents, not considered in these calculations, should be also estimated.

We compared our cross sections with those obtained in the EFT [74, 75] in terms of the constant  $L_{1,A}$ . Our values of the constant  $L_{1,A}$  are somehow smaller than its value obtained in the analysis of Refs. [75, 80], but in a good agreement with the dimensional analysis and with the data analysis [105, 106]. The comparison of the cross sections for the reactions in the neutral current channel and for the reaction (4.4) shows that they are described by both the potentials models and the pionless EFT with an accuracy better than 3 %. For the reaction (4.3), the achieved accuracy is  $\approx 3.4$  %. In this case, abrupt changes in the EFT cross section in the interval  $7 < E_\nu < 12 \text{ MeV}$  appeared, whereas the cross sections obtained from the potential models are smooth.

Our exchange charge and current densities are obtained in a general reference frame in terms of individual nucleon coordinates. This is a good approximation in the considered energy region, since the estimated effect of the boost currents is negligible. For higher energies, the calculations of the observables by sandwiching the operators between the intrinsic wave functions require to go one step further: by analogy with the case of the electromagnetic exchange currents [117], the center-of-mass frame dependence should be separated. This will be done elsewhere.

## Acknowledgments

This work is supported in part by the grants GA ĀR 202/03/0210 and 202/06/0746, and by Ministero dell' Istruzione, dell' Universita e della Ricerca of Italy (PRIN 2003). We thank R. Machleidt, M. Rentmeester and S. Nakamura for the correspondence and J. Adam, Jr. for the discussions.

- 
- [1] J.F. Donoghue, E. Golowich, B.R. Holstein, Dynamics of the Standard Model (Cambridge University Press, Cambridge, 1992).
  - [2] S. Weinberg, The Quantum Theory of Fields, v. II (Cambridge University Press, Cambridge, 1996).
  - [3] S.L. Adler, R. Dashen, Current Algebras (W.A. Benjamin, New York, 1968).

- [4] V. De Alfaro, S. Fubini, G. Furlan, C. Rossetti, *Currents in Hadron Physics* (North-Holland/American Elsevier, Amsterdam–London/New York, 1973).
- [5] J.J. Sakurai, *Currents and Mesons* (University of Chicago Press, Chicago, 1967).
- [6] R.J. Blin–Stoyle, *Fundamental Interactions and the Nucleus* (North-Holland/American Elsevier, Amsterdam–London/New York, 1973).
- [7] M. Rho, D. Wilkinson, *Mesons in Nuclei* (North-Holland, Amsterdam, 1979).
- [8] M. Rho, G.E. Brown, *Comments Part. Nucl. Phys.* **10** (1981) 201 .
- [9] T. Ericson, W. Weise, *Pions and Nuclei* (Clarendon Press, Oxford, 1988).
- [10] J.D. Walecka, *Theoretical Nuclear and Subnuclear Physics* (Oxford University Press, Oxford, 1995).
- [11] J. Carlson, R. Schiavilla, *Rev. Mod. Phys.* **70** (1998) 743 .
- [12] S. Nakamura, T. Sato, S. Ando, T.-S. Park, F. Myhrer, V. Gudkov, K. Kubodera, *Nucl. Phys.* **A707** (2002) 561 .
- [13] M. Chemtob, M. Rho, *Nucl. Phys.* **A163** (1971) 1 .
- [14] K. Kubodera, J. Delorme, M. Rho, *Phys. Rev. Lett.* **40** (1978) 755 .
- [15] E.A. Ivanov, E. Truhlík, *Sov. J. Part. Nucl.* **12** (1981) 198 .
- [16] I.S. Towner, *Ann. Rev. Nucl. Part. Sci.* **36** (1986) 115 .
- [17] M. Kirchbach, E. Truhlík, *Sov. J. Part. Nucl.* **17** (1986) 93 .
- [18] I.S. Towner, *Phys. Rep.* **155** (1987) 263 .
- [19] J.-F. Mathiot, *Phys. Rep.* **173** (1989) 63 .
- [20] D.O. Riska, *Phys. Rep.* **181** (1989) 207 .
- [21] B. Frois, J.-F. Mathiot, *Comments Part. Nucl. Phys.* **18** (1989) 291 .
- [22] H.-U. Jäger, M. Kirchbach, E. Truhlík, *Nucl. Phys.* **A404** (1983) 456 .
- [23] S. Nozawa, K. Kubodera, H. Ohtsubo, *Nucl. Phys.* **A453** (1986) 645 .
- [24] P.A.M. Guichon, C. Samour, *Nucl. Phys.* **A382** (1982) 461 .
- [25] M. Kirchbach, D.O. Riska, K. Tsushima, *Nucl. Phys.* **A542** (1992) 616 .
- [26] I.S. Towner, *Nucl. Phys.* **A542** (1992) 631 .
- [27] E.K. Warburton, I.S. Towner, *Phys. Lett.* **B294** (1992) 1 ; E.K. Warburton, I.S. Towner, B.A. Brown, *Phys. Rev.* **C49** (1994) 824 .
- [28] D.F. Measday, *Phys. Rep.* **354** (2001) 243 .
- [29] T. Gorringer, H.W. Fearing, *Rev. Mod. Phys.* **76** (2003) 31 .
- [30] E. Truhlík, *Czech. J. Phys.* **B53** (2003) 689 .
- [31] W.-Y.P. Hwang, E.M. Henley, *Ann. Phys. (N.Y.)* **129** (1980) 47 .
- [32] W.-Y.P. Hwang, E.M. Henley, G.A. Miller, *Ann. Phys. (N.Y.)* **137** (1981) 378 .
- [33] E. Hadjimichel, G.I. Poulis, T.W. Donnelly, *Phys. Rev.* **C45** (1992) 2666 .
- [34] G.I. Poulis, *Few-Body Systems* **24** (1998) 139 .
- [35] L. Diaconescu, R. Schiavilla, U. van Kolck, *Phys. Rev.* **C63** (2001) 044007 .
- [36] B. Mosconi, P. Ricci, *Phys. Rev.* **C55** (1997) 3115 .
- [37] G. Küster, H. Arenhövel, *Nucl. Phys.* **A626** (1998) 911 .
- [38] E. Ivanov, E. Truhlík, *Nucl. Phys.* **A316** (1979) 437 .
- [39] J. Adam, Jr., Ch. Hajduk H. Henning, P.U. Sauer, E. Truhlík, *Nucl. Phys.* **A531** (1991) 623 .
- [40] E. Truhlík, F.C. Khanna, *Int. J. Mod. Phys.* **A10** (1995) 499 .
- [41] E. Ivanov, E. Truhlík, *Nucl. Phys.* **A316** (1979) 456 ; G.E. Dogotar, E.A. Eramzhyan, E. Truhlík, *Nucl. Phys.* **A326** (1979) 225 ; J. Hošek, E. Truhlík, *Phys. Rev.* **C23** (1981) 665 ; S. Ciechanowicz, E. Truhlík, *Nucl. Phys.* **A414** (1984) 508 ; J. Adam, Jr., E. Truhlík, S.

- Ciechanowicz, K.M. Schmitt, Nucl. Phys. **A507** (1990) 675 .
- [42] J.G. Congleton, E. Truhlík, Phys. Rev. **C53** (1996) 957 .
- [43] N. Tataru, Y. Kohyama, K. Kubodera, Phys. Rev. **C42** (1990) 1694 ; K. Kubodera, S. Nozawa, Int. J. Mod. Phys. **E3** (1994) 101 .
- [44] J. Carlson, D.O. Riska, R. Schiavilla, R.B. Wiringa, Phys. Rev. **C44** (1991) 619 ; R. Schiavilla *et al.*, Phys. Rev. **C58** (1998) 1263 ; L.E. Marcucci, R. Schiavilla, M. Viviani, A. Kievsky, S. Rosati, J.F. Beacom, Phys. Rev. **C63** (2000) 015801 .
- [45] K. Tsushima, D.O. Riska, Nucl. Phys. **A549** (1992) 313 .
- [46] S.M. Ananyan, Phys. Rev. **C57** (1998) 2669 .
- [47] J. Schwinger, Ann. Phys. (N.Y.) **2** (1957) 407 ; M. Gell-Mann, M. Lévy, Nuovo Cim. **16** (1960) 705 .
- [48] S.M. Ananyan, B.D. Serot, J.D. Walecka, Phys. Rev. **C66** (2002) 055502 .
- [49] V. Dmitrašinović, Phys. Rev. **C54** (1996) 3247 .
- [50] F.C. Khanna, E. Truhlík, Nucl. Phys. **A673** (2000) 455 .
- [51] J. Smejkal, E. Truhlík, H. Göller, Nucl. Phys. **A624** (1997) 655 .
- [52] S. Weinberg, Phys. Rev. **166** (1968) 1568 ; S. Coleman, J. Wess, B. Zumino, Phys. Rev. **177** (1969) 2239 ; C.G. Callan, S. Coleman, J. Wess, B. Zumino, Phys. Rev. **177** (1969) 2247 .
- [53] J. Wess, B. Zumino, Phys. Rev. **163** (1967) 1727 ; J. Schwinger, Phys. Lett. **B24** (1967) 473 ; P. Chang, F. Gürsey, Phys. Rev. **164** (1967) 1752 ; B.W. Lee, H.T. Nieh, Phys. Rev. **166** (1968) 1507 ; S. Gasiorowicz, D.A. Geffen, Rev. Mod. Phys. **41** (1969) 531 .
- [54] V.I. Ogievetsky, B.M. Zupnik, Nucl. Phys. **B24** (1970) 612 .
- [55] U.-G. Meissner, Phys. Rep. **161** (1988) 213 .
- [56] M. Bando, T. Kugo, K. Yamawaki, Phys. Rep. **164** (1988) 217 .
- [57] J. Smejkal, E. Truhlík, nucl-th/9811080.
- [58] J. Adam, Jr., E. Truhlík, D. Adamová, Nucl. Phys. **A494** (1989) 556 .
- [59] H. Göller, H. Arenhövel, Few-Body Systems **13** (1992) 117 .
- [60] I. Sick, Prog. Part. Nucl. Phys. **47** (2001) 245 .
- [61] R. Gilman, F. Gross, J. Phys. **G28** (2002) R37 .
- [62] B. Mosconi, P. Ricci, E. Truhlík, Eur. Phys. J. **A25** (2005) 283 .
- [63] S. Weinberg, Physica **96A** (1979) 327; J. Gasser, H. Leutwyler, Ann. Phys. (N.Y.) **158** (1984) 142 ; Nucl. Phys. **B250** (1985) 517 .
- [64] V. Bernard, U.-G. Meissner, N. Kaiser, Int. J. Mod. Phys. **E4** (1995) 193 .
- [65] T.R. Hemmert, B.R. Holstein, J. Kambor, J. Phys. **G24** (1998) 1831 .
- [66] D.B. Kaplan, M.J. Savage, M.B. Wise, Nucl. Phys. **B478** (1996) 629 ; Phys. Lett. **B424** (1998) 390 .
- [67] T.-S. Park, K. Kubodera, D.-P. Min, M. Rho, Nucl. Phys. **A684** (2001) 101c ; M.J. Savage, Nucl. Phys. **A721** (2003) 94 ; U.-G. Meissner, V. Bernard, E. Epelbaum, W. Glöckle, nucl-th/0301079; J. Bijnens, U.-G. Meissner, A. Wirzba, hep-ph/0201266; J. Dobaczewski, nucl-th/0301069.
- [68] T.-S. Park, D.-P. Min, M. Rho, Phys. Rep. **233** (1993) 341 .
- [69] T.-S. Park, I.S. Towner, K. Kubodera, Nucl. Phys. **A579** (1994) 381 .
- [70] T.-S. Park, K. Kubodera, D.-P. Min, M. Rho, Astrophys. J. **507** (1998) 443 .
- [71] T.-S. Park, L.E. Marcucci, R. Schiavilla, M. Viviani, A. Kievsky, S. Rosati, K. Kubodera, D.-P. Min, M. Rho, Phys. Rev. **C67** (2003) 055206 .
- [72] S. Ando, T.-S. Park, K. Kubodera, F. Myhrer, Phys. Lett. **B533** (2002) 25 .
- [73] S. Ando, Y.H. Song, T.-S. Park, H.W. Fearing, K. Kubodera, Phys. Lett. **B555** (2003) 49 .

- [74] M. Butler, J.-W. Chen, Nucl. Phys. **A675** (2000) 575 .
- [75] M. Butler, J.-W. Chen, X. Kong, Phys. Rev. **C63** (2001) 035501 .
- [76] U.-G. Meissner, G. Smith, hep-ph/0011277.
- [77] T. Fuchs, M.R. Schindler J. Gegelia, S. Scherer, Phys. Lett. **B575** (2003) 11 .
- [78] D.O. Riska, Prog. Part. Nucl. Phys. **11** (1984) 9 .
- [79] J. Adam, Jr., E. Truhlík, P.U. Sauer, Czech. J. Phys. **B36** (1986) 383 .
- [80] S. Nakamura, T. Sato, V. Gudkov, K. Kubodera, Phys. Rev. **C63** (2001) 034617 .
- [81] S. Ying, W.C. Haxton, E.M. Henley, Phys. Rev. **C45** (1992) 1982 .
- [82] B. Mosconi, P. Ricci, E. Truhlík, nucl-th/0212042.
- [83] J.L. Friar, Phys. Rev. **C22** (1980) 796 .
- [84] F. Akram, H. Rashid, hep-ph/0403006.
- [85] SNO Collaboration, Phys. Rev. Lett. **87** (2001) 071301 ; Phys. Rev. Lett. **89** (2002) 011301 .
- [86] SNO Collaboration, nucl-ex/0309004.
- [87] A.W.P.Poon, nucl-ex/0312001.
- [88] B. Aharmim *et al.* Phys. Rev. **C72** (2005) 055502 .
- [89] J.D. Walecka, Semi-leptonic weak interactions in nuclei, in Muon physics, eds. V.W. Hughes, C.S. Wu, Academic Press, New York, 1972.
- [90] J.S. O'Connell, T.W. Donnelly, J.D. Walecka, Phys. Rev. **C6** (1972) 719 .
- [91] J.M. Blatt, L.C. Biedenharn, Phys. Rev. **86** (1952) 399 .
- [92] S. Eidelman *et al.*, Phys. Lett. **B592** (2004) 1 .
- [93] R. Machleidt, Adv. Nucl. Phys. **19** (1989) 189 .
- [94] P. Obersteiner, W. Plessas, E. Truhlík, in Proceedings of the XIII International Conference on Particles and Nuclei, Perugia, Italy, June 28–July 2, 1993, ed. A. Pascolini, World Scientific, Singapore, 1994, p.430.
- [95] V.G.J. Stoks, R.A.M. Klomp, C.P.F. Terheggen, J.J. de Swart, Phys. Rev. **C49** (1994) 2950 .
- [96] R. Davidson, N.C. Mukhopadhyay, R. Wittman, Phys. Rev. **D43** (1991) 71 .
- [97] R.B.Wiringa, V.G.J.Stoks, R.Schiavilla, Phys. Rev. **C51** (1995) 38 .
- [98] S. Hirschi, E. Lomon, N. Spencer, Comp. Phys. Comm. **9** (1975) 11 .
- [99] M. Rentmeester, personal communication, 2004.
- [100] R. Machleidt, Phys. Rev. **C63** (2001) 024001 .
- [101] J.R. Bergervoet, P.C. van Campen, W.A. van der Sanden, J.J. de Swart, Phys. Rev. **C38** (1988) 15 .
- [102] R. Machleidt, I. Slaus, J. Phys. **G27** (2001) R69 .
- [103] G.F. de Téramond, B. Gabioud, Phys. Rev. **C36** (1987) 691 .
- [104] B. Mosconi, P. Ricci, E. Truhlík, nucl-th/0507029.
- [105] A.B. Balantekin, H. Yüksel, Int. J. Mod. Phys. **E14** (2005) 39 .
- [106] M. Butler, J.-W. Chen, P. Vogel, Phys. Lett. **B549** (2002) 26 .
- [107] L.E. Marcucci, R. Schiavilla, S. Rosati, A. Kievsky, M. Viviani, Phys. Rev. **C66** (2002) 054003 .
- [108] V. Pascalutsa, Phys. Lett. **B503** (2001) 85 .
- [109] J. Smejkal, E. Truhlík, Phys. Rev. **C72** (2005) 015501 .
- [110] T.-Y. Saito, Y. Wu, S. Ishikawa, T. Sasakawa, Phys. Lett. **B242** (1990) 12 .
- [111] S. Nakamura, personal communication, 2003.
- [112] E. Blucher *et al.*, hep-ph/0512039.

- [113] W.J. Marciano, A. Sirlin, Phys. Rev. Lett. **96** (2006) 032002 .  
 [114] R. Machleidt, personal communication, 2004.  
 [115] F. Coester, D.O. Riska, Ann. Phys. (N.Y.) **234** (1994) 141 .  
 [116] W. Jaus, W.S. Woolcock, Helv. Phys. Acta **57** (1984) 644 .  
 [117] J. Adam, Jr., H. Arenhövel, Nucl. Phys. **A614** (1997) 289 .

## APPENDIX A: DEFINITIONS AND NOTATIONS

We use the Pauli metrics. The free nucleon spinors are normalized according to

$$u^+(p)u(p) = v^+(p)v(p) = 1. \quad (\text{A1})$$

The spinors are

$$u(p) = \sqrt{\frac{E(\vec{p}) + M}{2E(\vec{p})}} \begin{pmatrix} 1 \\ \frac{\vec{\sigma} \cdot \vec{p}}{E(\vec{p}) + M} \end{pmatrix}, \quad v(p) = \sqrt{\frac{E(\vec{p}) + M}{2E(\vec{p})}} \begin{pmatrix} \frac{\vec{\sigma} \cdot \vec{p}}{E(\vec{p}) + M} \\ 1 \end{pmatrix}. \quad (\text{A2})$$

The nucleon propagator is split into the positive- and negative frequency parts as follows

$$S_F(p) = -\frac{1}{i \not{p} + M} \equiv S_F^{(+)}(p) + S_F^{(-)}(p), \quad (\text{A3})$$

where

$$S_F^{(+)}(p) = \frac{1}{p_0 - E(\vec{p})} u(p)\bar{u}(p), \quad S_F^{(-)}(p) = \frac{1}{p_0 + E(\vec{p})} v(-p)\bar{v}(-p). \quad (\text{A4})$$

For a weak semileptonic reaction in the two-nucleon system NN,

$$NN(P_i) + l_i(p_i) \longrightarrow NN(P_f) + l_f(p_f), \quad (\text{A5})$$

we write the field-theoretical S-matrix element in the form

$$S = i(2\pi)^4 \delta^{(4)}(P_f + p_f - P_i - p_i) \tilde{l}_\mu(0) W_\mu^a(q), \quad (\text{A6})$$

where the matrix element of the lepton weak current is

$$\tilde{l}_\mu(0) = \langle l_f, p_f | l_\mu(0) | l_i, p_i \rangle, \quad (\text{A7})$$

the weak hadron current consists of the weak vector and weak axial vector parts,

$$W_\mu^a(q) = J_\mu^a(q) + J_{5\mu}^a(q), \quad (\text{A8})$$

and the momentum transfer  $q = p_i - p_f = P_f - P_i$ . In what follows, we deal only with the weak axial hadron current  $J_{5\mu}^a(q)$ .

We define the potentials and quasipotentials in a similar way, as it is done in Appendix A of Ref. [58].

We discuss next how the operator of a weak axial nuclear current  $j_{5\mu}^a$ , used in conjunction with the equation describing our NN system, can be related to the field-theoretical current  $J_{5\mu}^a(q)$ . Let the time evolution of the NN system be described by a Hamiltonian  $H = T + V$ ,

where  $T$  is the kinetic energy and  $V$  is the nuclear potential, which we take as the sum of the OBEs,

$$V = \sum_{B=\pi,\rho,\omega,a_1\dots} V_B. \quad (\text{A9})$$

If the nuclear physics calculations, based on the current  $j_{5\mu}^a$  and on the eigenfunctions of the Hamiltonian  $H$  should reflect the PCAC, then the current should satisfy the continuity equation

$$\vec{q} \cdot \vec{j}_5^a(\vec{q}) = [H, \rho_5^a(\vec{q})] + if_\pi m_\pi^2 \Delta_F^\pi(q^2) m^a(\vec{q}), \quad (\text{A10})$$

where  $m^a$  is the associated pion absorption amplitude. Supposing that the current consists of the one- and two-nucleon components, this equation splits into the following set of equations

$$\vec{q}_i \cdot \vec{j}_5^a(1, \vec{q}_i) = [T_i, \rho_5^a(1, \vec{q}_i)] + if_\pi m_\pi^2 \Delta_F^\pi(q^2) m^a(1, \vec{q}_i), \quad i = 1, 2, \quad (\text{A11})$$

$$\begin{aligned} \vec{q} \cdot \vec{j}_5^a(2, \vec{q}) &= [T_1 + T_2, \rho_5^a(2, \vec{q})] + ([V, \rho_5^a(1, \vec{q})] + (1 \leftrightarrow 2)) \\ &+ if_\pi m_\pi^2 \Delta_F^\pi(q^2) m^a(2, \vec{q}). \end{aligned} \quad (\text{A12})$$

In Eq. (A12), we neglected  $\rho_5^a(2, \vec{q})$  in the second commutator on the right hand side. Taking into account that  $q_0 = q_{10} + q_{20}$ , we find that Eqs.(3.7) and (A12) are in the full correspondence in the space of the nuclear states, that are described by the eigenfunctions of the Hamiltonian  $H$ . So we can consider the current  $j_{5\mu, B}^a(2)$ , defined in Eq. (3.1), as the WANEC of the range B.

## APPENDIX B: THE WANECs OF THE $\sigma$ MESON RANGE

Realistic OBEs contain standardly the  $\sigma$  meson exchange, describing the attraction at medium distances. On the other hand, our WANECs do not contain the component due to this exchange so far. This is due to the fact that our Lagrangians reflect the non-linear chiral symmetry and it is not clear how to include the  $\sigma$  meson into the scheme consistently. Here we construct the axial exchange current of the  $\sigma$  range starting from a Lagrangian

$$\Delta\mathcal{L} = g_\sigma \bar{N}N \phi + i \frac{g_A}{f_\pi} g_\sigma \bar{N} \gamma_5 (\vec{\tau} \cdot \vec{\pi}) N \phi + ig_{\pi NN} \bar{N} \gamma_5 (\vec{\tau} \cdot \vec{\pi}) N + ig_A g_\rho \bar{N} \gamma_\nu \gamma_5 (\vec{\tau} \cdot \vec{a}_\nu) N, \quad (\text{B1})$$

where besides the pseudoscalar  $\pi NN$  coupling standardly accepted  $\sigma NN$  coupling is present. The relativistic amplitudes derived from this Lagrangian by analogy with Sect. II for other exchanges of our model are the nucleon Born amplitude  $J_{5\mu, \sigma}^a$  and the only potential contact term  $J_{5\mu, c\sigma}^a(\pi)$ . It can be verified that these amplitudes satisfy the PCAC equation

$$q_\mu [J_{5\mu, \sigma}^a + J_{5\mu, c\sigma}^a] = if_\pi m_\pi^2 \Delta_F^\pi(q^2) [M_\sigma^a + M_{c\sigma}^a]. \quad (\text{B2})$$

Using the methods developed in Sect. III, we obtain the pair term of the  $\sigma$  range

$$\vec{j}_{5, \sigma}^a(pair) = ig_A F_A \frac{g_\sigma^2}{(2M)^3} [\vec{q}_2 \times (\vec{P}_1 + \vec{q}) + i \vec{P}_1 \times (\vec{\sigma}_1 \times \vec{q})] \tau_1^a \Delta_F^\sigma(\vec{q}_2^2) + (1 \leftrightarrow 2) \quad (\text{B3})$$

$$j_{50, \sigma}^a(pair) = g_A F_A \frac{g_\sigma^2}{(2M)^2} (\vec{\sigma}_1 \cdot (\vec{P}_1 + \vec{q})) \tau_1^a \Delta_F^\sigma(\vec{q}_2^2) + (1 \leftrightarrow 2). \quad (\text{B4})$$

For the transition  ${}^3S_1 - {}^3D_1 \rightarrow {}^1S_0$ , only the second term at the right hand side of the space component of the current  $\vec{j}_{5, \sigma}^a(pair)$  contributes. However, being proportional to  $\vec{q}$ , it is of little importance at the threshold. In contrast to the current  $\vec{A}_\pm(S)$  presented in Eq. (2.5a) of the Ref. [45], our current (B3) does not contain the spurious term analogous to  $-\vec{\sigma}_1 \vec{k}^2/4$ .